Characterization of the Immune Stimulated Release of Extracellular Vesicles from Murine Cells

Andrew Norrie

A Thesis Submitted in Partial Fulfillment of the Requirements for the Master's Degree in Biochemistry, Microbiology, and Immunology.

Dr. Marc-André Langlois

Department of Biochemistry Microbiology & Immunology
Faculty of Medicine
University of Ottawa

Abstract

Introduction: Viruses, extracellular vesicles (EVs) and endogenous retroviruses (ERVs) are types of sub-micron particles which are known to be released from a vast range of cell types, across many species. There are many medically relevant sub-micron particles which can enter healthy cells and enable the intercellular delivery of functional host-derived and foreign products, through their enclosed lipid layers. While multiple particle subsets have been identified, many of the properties, behaviors and biochemical functions have not been fully described and have yet to be characterized.

Materials and Methods: $CD4^+$ naïve T-cells were isolated from female C57BL6/N mice and stimulated with varying concentrations of PMA/I. In addition to concentration, the length of PMA/I activation was assessed. Supernatants and cells were harvested, filtered, and stained to be subsequently analyzed by Nanoscale Flow Cytometry, Nanoparticle Tracking Analysis and Flow Cytometry. Particle populations were quantified and sorted by size, by NTA. Labelling dye CFSE was used in conjunction with fluorescently conjugated CD81 and CD9 antibodies to separate EVs, including exosomes, from background signal. Naïve T-cell purity, viability and levels of activation were assessed by flow cytometry using CD3, CD4 and CD62L antibodies and viability staining.

Results: Increasing PMA concentration led to a global increase in particles by T-cells and a specific increase in smaller particle production and were demonstrated to be significant by Welch's T-test, when compared to non-activated and DMSO controls ($p<0.0001$). In addition to concentration, activation length also correlated

with increases in total particle counts and a specific increase in the secretion of smaller particles in comparison to non-activated and DMSO controls ($p<0.0001$). Labelling techniques by NFC revealed an increased presence of CFSE-CD81 positive and CFSE-CD9 positive particles secreted by T-cells, treated for 24 hours, compared to the 0- and 12-hour timepoints.

Conclusion: This work demonstrates preliminary steps and outlines methods to begin assessing discrete particle populations and subsets secreted by murine naïve T-cells. Being able to identify patterns of particle secretions by naïve T-cells, especially under immune-stimulated conditions, may be the solution to uncovering the necessary information on EV physiology, that is required to understand the roles EVs play in pathology and how these conserved pathways may lead conditions to become exacerbated. This knowledge is essential to uncovering the roles EVs play in pathophysiology, and in the development of novel rapid diagnostic tests, to screen for cancers, infections, autoimmune disorders, and numerous other pathological conditions.

Acknowledgements

First and foremost, I would like to thank Dr. Marc-André Langlois for providing the opportunity to be a contributing member of his research team where I was able to apply theoretical scientific study, in a practical laboratory environment, and acquire niche specialized scientific skills that I would not have been able to perform without his mentoring.

Secondly, I would like to thank my family. My parents and my brother for their everlasting support, continued exceptionally valuable guidance and seemingly clairvoyant wisdom as well as their unconditional love. You have all been there to encourage, inspire and empower me throughout my pursuit of education and scientific proficiency.

A special thanks to all the members of the Langlois research team for their contributions to an exceptionally positive work environment and their assistance throughout my Master's journey. Thank you, Dr. Tyler Renner, for showing me the ropes and developing the necessary skills to set me up for success for my degree, for your guidance, and for our informative discussions. Thank you to Anna Fritzche for sharing your knowledge and instruction which contributed significantly to the development of my lab skills. To my lab colleagues, Matthew Greig, Mariam Maltseva, Ricardo Mojica, Tasneem Abbas and Yannick Galipeau, thank you for your cooperation, support, assistance and friendship along the way, I could not have done it without your support.

I would like to thank all my friends as they were always right there to provide me with support, advice, camaraderie, laughter, and so much more. Thank you, I will always cherish your kindnesses and support.

Thank you to the Faculty and Staff who have aided, taught, guided and challenged me throughout the course of my graduate education. Dr. Vera Tang, for teaching me the skills, theories and the immense power of flow cytometry. Thank you to Dr. Martin Pelchat for his coaching and mentoring, as a member of my TAC, and providing me immensely useful and applicable skills using R software. Thank you, Dr. Dylan Burger, for assisting me throughout my project's development, challenging me and mentoring me, as a member of my TAC, and teaching and providing me with the knowledge and technical skills to operate the Zeta View. I would like to also thank Dr. Marceline-Côté and Dr. Subash Sad for developing my scientific literacy and academic skills. To the ACVS staff, thank you for taking the time to provide training, help and assistance with caring for our animal models. A big thank you to the faculty Technical Support Team for their role in my training and providing me with assistance whenever I encountered issues.

Additionally, I would like to thank Dr. Raymund Wellinger and his team at the Université de Sherbrooke for developing my necessary theoretical and technical scientific skills to commence my graduate education. Finally, my sincerest thanks to Dr. Virginia Stroeher at Bishop's University for invoking my scientific curiosity in Microbiology with lectures and continued support and assistance throughout my honour's specialization program.

Thanks to BioRender.com for providing the platform and assets to develop high resolution illustrative figures and graphics under an Academic License, figures were exported under a paid subscription.

Table of Contents

List of Tables

List of Figures

List of Abbreviations

AAA-ATPase: ATPases Associated with diverse cellular Activities

ATPase: a group of enzymes which hydrolyze ATP

Alix: ALG-2 interacting protein X

A-MLV: Amphotropic Murine Leukemia Virus

ATP: Adenosine Triphosphate

CAT-1: Cationic amino acid transporter 1

CCR5: C-C chemokine receptor type 5

CD4: Cluster of Differentiation 4

CD43: Cluster of Differentiation 43

CD62L: Cluster of Differentiation 62L or L-Selectin

CD63: Cluster of Differentiation 63

CD69: Cluster of Differentiation 69

CD81: Cluster of Differentiation 81

CD82: Cluster of Differentiation 83

CD9: Cluster of Differentiation 9

cDNA: Complementary DNA

CFSE: Carboxyfluoresceinsuccinimidyl ester

CXCR4: C-X-C Chemokine Receptor Type 4

DMSO: Dimethyl Sulfoxide

E-MLV: Ecotropic Murine Leukemia Virus

Env: Envelope Glycoprotein

ERV: Endogenous Retrovirus

ESCRT: Endosomal Sorting Complexes Required for Transport

EV: Extracellular vesicles

FBS: Fetal Bovine Serum

Gag: Group-specific antigen

GTP: Guanosine Triphosphate

HERV: Human Endogenous Retrovirus

HERV-K: Human Endogenous Retrovirus Type K

HIV: Human Immunodeficiency Virus

HML: Human MMTV-like Subclass

ICAM1: Intracellular Adhesion Molecule 1 or Cluster of Differentiation 54

IL-2: Interleukin-2

ILV: Intraluminal Vesicle

ISG15: Interferon Stimulated Gene 15

JAK: Janus Kinase

LE: Late Endosome

LFA1: Lymphocyte Function-associated Antigen 1

LINES: Long-Interspersed Nuclear Element

LTR: Long Terminal Repeat

MHC-I: Major Histocompatibility Complex 1

miRNA: Micro RNA

MLV: Murine Leukemia Virus

mRNA: Messenger RNA

MVB: Multivesicular Bodies

MVE: Multivesicular Endosome

NFC: Nanoscale Flow Cytometry

NF-κB: Nuclear Factor Kappa-Light-Chain-Enhancer of Activated B cells

NTA: Nanoparticle Tracking Analysis

Pit1: Sodium-dependent Phosphate Transporter 1

Pit2: Sodium-dependent Phosphate Transporter 2

PMA/I: Phorbol 12-Myristate 13-acetate and Ionomycin

P-MLV: Polytropic Murine Leukemia Virus

Pol: Polymerase

PS: Phosphatidylserine

Rab 5: Ras-related Protein Rab-5a

GTPase: a group of enzymes which hydrolyze GTP

RPS: Resistive Pulse Sensing

SEC: Size Exclusion Chromatography

SINES: Short-interspersed Nuclear Element

SNAP: Soluble NSF Attachment proteins

STAT: Signal Transducer and Activator of Transcription Proteins

TEM: Transmission Electron Microscopy

Th1: T-helper type 1

Th2: T-helper type 2

Th17: T-helper type 17

Tn: Naïve T-cell

TNF: Tumor Necrosis Factor

TNFα: Tumor Necrosis Factor Alpha

TRPS: Tunable Resistive Pulse Sensing

TSG101: Tumor Susceptibility Gene 101

t-SNARE: Target-SNAP Receptor

SNARE: SNAP Receptor

VLP: Virus-like Particle

v-SNARE: Vesicle SNAP Recpetor

Vsp4: Vesicle-fusing ATPase

X-MLV: Xenotropic Murine Leukemia Virus

XPR1: Xenotropic and Polytropic Retrovirus Receptor 1

Introduction

Viruses, extracellular vesicles, and endogenous retroviruses are different categories of biological particles secreted from a vast range of cells across many species[1,2]. The secretion of these particles enables the cell-to-cell transfer of different biological cargoes which can lead to the delivery of foreign and host-derived biological macromolecules, modulation of recipient cell behaviour, infections, disease progression and pathologies[3]. Viruses, extracellular vesicles and endogenous retroviruses share many similarities in biochemical/biophysical composition but vary vastly in their mechanisms of secretion and cellular entry/uptake[4,5].

Biological microparticles and nanoparticles such as viruses, extracellular vesicles and endogenous retroviruses have been well described. However, cell-stimulated mechanisms of secretion, behaviour and precise differentiation remain to be reported, particularly in heterogenous populations of particles.

In this proposed study, we sought to identify and categorize the heterogenous populations of microparticles released from murine cells under distinct immune stimulating condition(s).

Through modern quantitative techniques such as Nanoscale Flow Cytometry (NFC), and Nanoparticle Tracking Analysis (NTA), we analyzed the observed distributions of cell-secreted particles following a stimulus. With this research, we hope to further modern medical screening techniques and practices by correlating specific microparticle egress patterns with identified diseases and infections, which would

ultimately serve as a swift diagnostic and prognostic marker of many diseases including immune-evasive diseases.

Literature Review

Cell Secreted Biological Sub-micron Particles

Cells are known to secrete a plethora of different biological products from metabolic by-products to cell-specific accessory proteins to cell derived vesicles[6]. Several cell-secreted particles enable the successful cell-to-cell delivery of both foreign and host-derived cargo which is necessary for cell survival and intercellular communication[2]. However, under certain conditions, cell-derived particle secretions may contribute to cellular dysfunction, pathology and disease[3]. Viruses are some of the most notable cell-secreted particles which contribute to pathology and disease[7]. However, in the rapidly expanding fields of extracellular vesicles and endogenous retroviruses, there is mounting evidence correlating their secretion and efficient cellular uptake with many pathologies, diseases and disorders[8–10].

Viruses are a diverse and expansive taxonomic classification of obligate intracellular pathogens[11]. Viruses require host cells in order to replicate and propagate. Viral entry into host cells is determined by the host tropism of a virus. The ability of a virus to bind to highly specific host cell receptors, or more broad conserved surface receptors, will determine their entry into specific hosts, host tissues and range of susceptible organisms[12]. Viral egress or secretion varies between classes of viruses. Viruses will take advantage of host cell machinery to replicate and will be released through direct lysis of the host cell or through a slower latent state in which the host cell is not lysed, following viral replication, and allows progressive secretion of viruses[13]. Latency is typically achieved through incorporation of the viral genome into

the host's genome where it remains sheltered and protected from host-restriction factors, and in some cases an immune system, all while enabling viral replication to occur[13]. Some of the most notable viruses, which integrate into the host cell genome, are the *Retroviridae* and *Herpesviridae* families of viruses[14].

One highly conserved property of cells, across all three domains of life, is their inherent ability to shed and secrete particles, more specifically extracellular vesicles[15]. In addition to metabolic by-products and cell-associated proteins, which comprise the secretome, cells expel small spherical lipid bodies called extracellular vesicles[1]. Extracellular vesicles (EVs) are very heterogeneous[16]. The size of their lipid bilayer can vary which directly influences the amount and/or size of potentially enclosed biological cargoes, as well as the abundance of lipid-associated surface proteins[17]. The term extracellular vesicle encompasses a vast range of shed or secreted vesicles which are often difficult to differentiate due to their structural similarities and biochemical properties, thus EVs were further sub-divided into three classifications of cell-derived vesicles. The three main classifications of extracellular vesicles are apoptotic bodies, microvesicles, and exosomes[18]. Each classification is used to differentiate cell-derived vesicles based on size, cellular origin/egress pathway, and by enclosed biological cargoes[19].

Retroviruses & Endogenous Retroviruses

The *Retroviridae* family of viruses represent an assembly of viruses which infect cells and integrate their genetic material into the host cell genome[20]. These types of

retroviral infections are a detriment to host cell survival, healthy cell behaviour, multicellular host immune systems and a quandary in modern medicine[21].

Retroviruses are spherical, positive sense single-stranded RNA viruses which are surrounded by a phospholipid bilayer envelope and roughly 100nm in total diameter[22]. Retroviral particles are comprised of several main components: an RNA genome which conserves the hereditary potential of the virus; nucleocapsid proteins which bind and surround the nucleic acid; a protein capsid core necessary for the structural integrity of the virus; matrix proteins which bind the capsid core to the surrounding envelope; virally encoded reverse transcriptase and integrase enzymes which serve to convert the RNA genome into a DNA intermediate and to physically fuse the DNA intermediate into the host's DNA genome; a phospholipid bilayer acquired from budding from the surface of a host cell; viral surface glycoproteins which enable host cell binding; and, in some instances, host restriction factors which inhibit and cripple host defense mechanisms against viral infection[23].

Retroviridae includes three main subfamilies: (i) oncogenic retroviruses (*Alpha*, *Beta*, *Delta*, *Epsilon & Gamma retrovirus*); (ii) latent/longstanding viruses *Lentivirus;* and (iii) foamy viruses *Spumaretrovirinae*[24]. Some of the most notable retroviruses are murine leukemia virus (MLV), mouse mammary tumor virus, human immunodeficiency virus (HIV1/2) and human T-lymphotropic virus[24].

Successful retroviral infections begin through specific receptor mediated binding of their surface glycoprotein to a host-cell receptor[25]. Following receptor binding on the host cell's surface, conformational changes to the env glycoprotein are induced which leads to the creation of a pore within the viral envelope to fuse the viral

envelope with that of the host cell membrane[26,27]. The resulting fusion of the host and viral membranes leads to the entry of the viral core and associated enclosed viral contents within the host cell's cytoplasm[28]. Within the cytoplasm, the retroviral core undergoes the uncoating process which removes and disassembles the protein capsid surrounding the viral genome[25]. The uncoating process enables the RNA-based viral genome to be converted into a DNA intermediate, in a process called reverse transcription, which is facilitated by the viral-encoded reverse transcriptase enzyme[29]. During the reverse transcription process, host proteins, accessory proteins, and essential proteins for retroviral integration, such as the integrase enzyme, amalgamate to form pre-integration complexes[29]. The pre-integration complexes are necessary for trafficking to and within the nucleus of the cell, which precedes the integration process of the cDNA viral genome intermediate into the host genome[30]. The ability of a retrovirus to permeate the nuclear membrane varies between retroviruses. Some retroviruses, such as HIV, can be imported into the nucleus through manipulation of nuclear active transport mechanisms[30]. While others, such as MLV, require more favourable conditions during cell division, in which the nuclear membrane is compromised and becomes more permeable, enabling viral pre-integration complexes access to host chromosomes[31].

One main advantage of retroviruses is their inherent ability to integrate a copy of their genetic material into a susceptible host genome[20]. After reverse transcribing their RNA genome into a cDNA intermediate the integrase enzyme facilitates the cleavage of the 3' ends of the cDNA forming "sticky ends" necessary for insertion in the host genome[20]. Once pre-integration complexes are trafficked to host chromatin

integrase additional facilitates a “cut and paste” mechanism of strand transfer by inserting the viral cDNA into the host chromatin by performing compatible cleavages on the host DNA[20]. The insertion of the viral cDNA into the host genome is aided by host encoded proteins DNA polymerase, Flap endonuclease and DNA ligase which together will complete the missing regions of DNA, remove excess incongruent 5’ cDNA strands and bind the cDNA and host strands together[20]. Once the viral DNA is integrated into the host genome, called a provirus, it will remain within the host genome as a permanent addition to the host and will replicate whenever the host cell does, preserving its genetic material for several generations[32]. While integrated, the infection is considered latent; however, this does not mean the virus is dormant, i.e. transcriptionally silent, and in fact can actively transcribe encoded genes at minimal levels which do not trigger host cell or immune cell defenses[33]. The degree to which proviruses can replicate may vary depending on the site of integration within DNA chromatin as well as chromatin organization and epigenetic modifications[32]. Over several generations of replications, integrated viruses may change through the accumulation of genetic mutations[34]. The accumulation of genetic mutations can be severe enough to inhibit or minimize the potential of provirus transcription which hinders their ability to mobilize and form fully intact and functional exogenous viruses[35]. This is how endogenous retroviruses (ERVs) are generated and will be discussed further[35].

Integrated proviruses mobilize to the extracellular environment following host transcription of the provirus DNA genome by host encoded RNA polymerase II. Transcription commences at the 5’ LTR within the R region. Several full-length RNA

transcripts are synthesized by encoding the entirety of the retroviral genome and modified at the 5' and 3' ends with a methylated cap and a polyadenylated tail, respectively[36]. The full-length RNA genomes, usually two copies, are encapsidated inside the budding virions[37]. Full-length RNA transcripts also serve as the template necessary in the translation of the *gag*, *pro* and *pol* genes into associated polyproteins by ribosomes in the cytoplasm[38,39]. The gag polyproteins (Gag-Pro, Gag-Pro-Pol) direct and assemble capsid particles, in conjunction with the additional virally encoded particles and copies of the genome, which are necessary functions for viral maturation, capsid stability and budding at the cell surface[40]. In addition to fully synthesized transcripts, transcribed provirus is alternatively spliced producing various transcripts of RNA which are used to generate the env proteins[41]. Spliced Env RNA transcripts are translated by ribosomes on the surface of the rough endoplasmic reticulum where they are additionally N- and O- glycosylated[42]. Env proteins are shuttled from the rough endoplasmic reticulum to the golgi apparatus and the Trans Golgi Network by vesicles[42]. Vesicles shuttle from the golgi apparatus to the plasma membrane where env proteins are inserted[42]. Env glycoproteins shuttle through the plasma membrane, through a process of lateral diffusion, from their insertion point in the plasma membrane to the site of budding where env proteins concentrate and are incorporated with gag polyproteins and copies of the RNA genome[42]. Retroviral particles preferentially bud from specific sites, within the plasma membrane, namely cholesterol rich lipid rafts and tetraspanin enriched microdomains[43,44]. Here, immature retroviral particles readily bud from the surface of the plasma membrane and are liberated to the extracellular environment where

they begin to mature[45]. Retroviral maturation requires gag polyproteins to be cleaved into independent protein components catalyzed by the virally encoded protease which enables the gag protein to form a fully intact capsid which surrounds the copies of the enclosed genomes[45].

In some cases, retroviruses may also reach the extracellular environment through other methods other than shedding from the plasma membrane. In some cases, HIV is capable of being released from cells via apoptosis[46].

Endogenous retroviruses are highly conserved regions of proviral DNA sequences, within host genomes, which resulted from a retroviral infection and successful integration into a host genome or germline cell[35,47]. As such, ERVs are passed down vertically to subsequent generations of offspring, differentiated cells or subsequent daughter cells[35,48]. Since the presence of ERVs are the result of a previous retroviral infection, they are also classified by their sequence similarity to the retroviral families which may have generated them[49]. Most ERVs, however, are non-functional in the sense they are not solely capable of producing a fully functioning virus which can mobilize to the extracellular environment[49]. The transcription of ERVs is determined by the host cells epigenetic, stress, disease and environmental factors[50,51]. Some ERVs lose their ability to function autonomously through the inevitable accumulation of mutations which are non-reversible[50]. ERVs are subjected to the existing mechanisms maintaining host genomes which inevitably result in the accumulation of mutations as time increases. Mutations in ERVs are acquired from many generations of cell division, transposition in the genome (deletions), discrepancies in cell division and DNA repair machinery during DNA breaks[52,53]. ERVs belong to the

retrotransposon class of transposable elements within host genomes and roughly constitutes ten percent of mouse and eight percent of human genomes[54,55]. Whereas in mice, many ERVs are actively transposing and transcribed, most of the human ERVs are inactive/extinct due to generations of acquired mutations and potent host restriction[54]. Retrotransposons are a Class I transposable element, containing the LINES, SINES and LTRs, which can change positions within a host genome, facilitated by transcription, and the reverse transcription by a reverse transcriptase to enable the expressed RNA to be converted into a DNA intermediate and inserted elsewhere in the genome[56]. Retroviruses are hypothesized to have evolved from the early LTR transposable element family called Gypsy like LTRs which are thought to have gained ENV glycoprotein functions enabling viral lifecycle functions[57]. Copies of endogenized viruses become amplified, and potentially acquire new mutations, upon transposition into new localizations within the genome[58]. Mutations acquired may be more beneficial for ERV replication and production or may hinder expression and/or the production of infectious particles[53].

In addition to the classifications of transposable elements, ERVs are further sub-classified into three different classes (Class I, Class II, and Class III) based on their lineage and sequence similarities to exogenous retrovirus counterparts[50]. Class I ERVs represent those which resemble the *Gammaretrovirus* and *Epsilonretrovirus* families of retroviruses. Class II ERVs represent a group of ERVs which closest resemble the *Alpha*, *Beta*, *Delta* and *Lentivirus* families. Finally, Class III ERVs represent those ERVs which are most similar to the *Spumaretrovirinae* family of viruses[49].

Class I ERVs are prevalent in several mice species, including laboratory strains, and contain many active and infectious members in their group closely related to the Murine Leukemia Virus (MLV) exogenous retroviruses[59]. There are many active members of Class I ERVs, which are not only capable of producing capsid and nucleocapsid proteins but also produce fully infectious particles and ERVs, which work together to increase replicative fitness and mobility from the genome to the extracellular environment[59]. Class I ERVs are often further sub-classified into different ERV "families" typically differentiated using polymerase chain reaction from several mouse strain preparations. The Class I ERVs were differentiated by their ENV sequences as these were determinants of host range for each Class I ERV, especially those belonging to the MLV ERVs[59]. These subclassifications are xenotropic (X-MLV), polytropic (P-MLV), amphotropic (A-MLV) and ecotropic (E-MLV)[59]. The X-MLVs can infect a vast range of susceptible mammalian cells, but do not infect lab strains of mice[60]. The X-MLVs require the XPR1 phosphate transporter to be on the host cell surface for successful viral entry[61]. As such, laboratory mouse strains are not susceptible to X-MLV infection as they possess mutations in their XPR1 receptor which are not conducive for X-MLV binding[61]. The P-MLVs have a less broad range of susceptible mammalian hosts, but also require the XPR1 receptor for viral entry[61]. However, P-MLVs do not produce full viral particles[59]. The A-MLVs can infect several mammals including humans and are commonly found in wild mouse preparations[26]. The A-MLVs take advantage of the Pit1 and Pit2 sodium dependent phosphate symporters for viral entry[62]. Finally, the E-MLVs are capable

of infecting mouse and rat populations, including laboratory strains, and require the CAT-1 cationic amino acid transporter for viral entry[26].

ERV production and mobilization differs depending on the subclass of ERV. The xenotropic and ecotropic subclasses of Class I ERVs produce infectious particles[59]. The ecotropic ERVs are the least abundant in wild and laboratory strains with roughly one copy per genome[59]. The xenotropic ERVs are more abundant than ecotropic ERVs with approximately 20 copies per mouse genome[59]. As previously mentioned, the polytropic ERVs are not solely capable of producing infectious particles and are the most abundant subclass of Class I ERVs, with approximately 30 copies per murine genome[59]. Polytropic ERVs, however, are capable of mobilizing to the extracellular environment by recombining with invading exogenous viruses and other ERV subclasses in a pseudo type manner [54,59,63]. While the transcription and production of exogenous ERV particles is dependent on cellular transcription rather than autonomous functions of the ERVs, external stimuli have an impact on cellular transcription and therefore ERV production in mice. In the work of Greenberger *et al.* 1975, the researchers demonstrate an increased production of X-MLVs following stimulation of spleen cells harvested from the BALB/c lab strain of mice with known pathogen associated molecular patterns lipopolysaccharide and concanavalin A[64]. This effect is not only native to murine immune cell subsets but is also exemplified with the human endogenous retrovirus HERV-K[65].

While most human endogenous retroviruses are non-transcriptionally active, one exception is the family HERV-K which can produce a full-length transcript and infectious particles[65]. These ERVs, which are also referred to as the human MMTV-

like subclass (HML), are the subject of a lot of research to determine their role in disease and disease progression[66]. Researchers have speculated that the env and accessory protein genes, comprising these HERVs, are oncogenic in nature and may lead to the development of tumors and autoimmune disorders[10]. It has been demonstrated that their expression also varies under different cell stimulating conditions, such as cancers, HIV-1 infections, and immune cell stimulants[11–13].

Extracellular Vesicles: Apoptotic bodies, Microvesicles & Exosomes

The term extracellular vesicle (EV) is an encompassing term for the heterogenous populations of small lipid bodies that shed or are secreted by cells and enable the cell-to-cell delivery of a variety of biological contents[69]. These lipid bodies include exosomes, microvesicles and apoptotic bodies[69]. Conventionally, while their biochemical compositions are almost identical in structure, researchers have used diameter, biological contents, mechanism of egress and surface markers as variables to segregate these discrete populations[8]. Extracellular vesicles are the subject of intense research for the potential roles they play in pathology, novel diagnostic, and potential therapeutic strategies[3,70].

Apoptotic bodies are the largest of the extracellular vesicles varying from 800nm-5000nm and, as the name suggests, are formed during apoptosis or programmed cell death when the cell membrane begins to bleb and fragment, into smaller fractions, in order to be efficiently cleared and removed by phagocytes of the immune system[3,71]. Apoptotic bodies are diverse, and typically house a variety of

host-derived biological cargoes in different densities and, due to their size, are able to retain larger structures such as genomic DNA, RNAs, proteins, lipids and mitochondrial derived contents[71,72]. Depending on the cell type, cells will bleb and form apoptotic bodies in different patterns, but all ultimately form a diverse range of apoptotic body subsets that differ in size and enclosed content[71]. There are many well described stimulators of apoptosis which transduce intrinsic and extrinsic apoptotic pathways such as DNA damage, bacterial and viral infections, hypoxia, Fas receptor ligand binding and activation of TNF receptors and the TNF signalling pathways to name a few[73]. In addition to intrinsic and extrinsic pathways, apoptosis can be induced by the immune system via cytotoxic T-lymphocytes. Once activated, effector T-cells such as cytotoxic T-lymphocytes will induce cell killing through specialized granules perforin and granzyme[74,75]. Together, perforin and granzyme will porate the plasma membrane and facilitate the break down of cellular contents, including proteins and chromatin[76]. Similarly, to the effector functions of cytotoxic T-lymphocytes, Natural Killer cells will also perform the same site directed cell killing via the release of perforin and granzyme protease[77].

One feature of apoptotic bodies, which enables their discrimination from other EVs, is the presence of phosphatidylserine (PS) and annexin V in conjunction with the size of the particle[78]. The presence of PS on the outer surface of the plasma membrane of a cell is a typical stage of apoptosis in which the asymmetry of lipoproteins are no longer maintained by cellular flippase, floppase and scramblase enzymes[79,80]. Annexin V is one of many annexin proteins which all bind membrane receptors in a calcium (Ca^{2+}) dependent fashion[81]. Annexin V is well known for its

affinity to bind PS on the surface of apoptotic cells[81]. These processes precede individual apoptotic body formation and, therefore, maintain their presence on the surface of apoptotic bodies; thus, enabling their identification[80].

Microvesicles are a second classification of EV which range in sizes of 100nm-1000nm[8]. Microvesicles are differentiated from other EVs by their size and their ability to readily shed from the plasma membrane at lipid raft junctions[82]. Microvesicles curve outward from the cytosol and are stimulated by the presence of calcium[83]. Increases in cellular calcium levels lead to the activation of calcium dependent proteases and actin binding protein gelsolin which facilitates the detachment of the cell membrane from the cytoskeleton network, via cleavage of membrane bound proteins with cytoskeletal filaments, and the disassembly of actin filaments respectively[8]. Microvesicles are smaller than apoptotic bodies. As such, the encapsulated cargoes are comprised of smaller molecules like proteins, RNAs and lipids[84]. Microvesicle release is stimulated under a plethora of conditions including: cellular activation, apoptosis, hypoxia, oxidative stress, shear stress, bacterial and viral infections, proinflammatory signals, cancers and many more conditions of pathology; however, many remain to be uncovered[8,85,86].

Exosomes are the smallest type of EV ranging from sizes of 30nm up to 100nm in diameter[3]. In addition to their small size, exosomes are differentiated from other EVs by their biogenesis and egress pathway. Exosomes biogenesis, trafficking and secretion are all affiliated with the cellular endomembrane system, endosomal sorting complex required for transport (ESCRT) pathways, and ESCRT independent pathways, including the tetraspanin family of transmembrane proteins and the

membrane lipid ceramide[8]. The endosomal system is a network of intracellular vesicles responsible for the recycling of cell surface proteins, the degradation of macromolecules such as proteins, solutes, and surface receptors through fusion with lysosomes, and sorting and trafficking cargo between both degradative and recycling pathways[87]. The term exosomes refers to internal vesicles called intraluminal vesicles (ILVs) which are secreted into the extracellular environment[88]. ILVs are externalized by cells into the extracellular space via fusion of larger encasing vesicles called multivesicular bodies or late endosomes (MVB/MVE/LEs), with the plasma membrane[88]. Vesicles from the plasma membrane are internalized via endocytic pathways (i.e., clathrin, caveolae pathways, micropinocytosis, etc.) and fuse with early endosomes and late endosomes (MVBs) which are mediated by ESCRT protein complexes[87,89,90]. There are four ESCRT proteins complexes (0, I, II, III) and the AAA ATPase – Vsp4 complex which work sequentially to bind, conglomerate and sort ubiquitinated cargo on endocytosed vesicles from the plasma membrane and facilitate their fusion with early and late endosomes generating ILVs within[90,91]. In the degradative pathway, MVBs fuse with lysosomes where ILVs and enclosed cargoes can be degraded[86,92]. MVBs may also fuse with the plasma membrane resulting in the release of exosomes and enclosed cargoes into the extracellular environment[88]. The trafficking of these vesicles, through the cytosol and fusion with the plasma membrane, is accomplished by a collection of proteins including the family of GTPases known as the Rab family of GTPases, SNAP and SNARE proteins, motor proteins, cytoskeletal filaments and Rab effectors or tethering factors[3,93]. Vesicles are pulled along the network of cytoskeletal

infrastructure, called microtubules, by motor protein family's kinesins and dyneins which anchor vesicles to microtubules and hydrolyze ATP to transport vesicles throughout the cell[94]. The membrane of endosomes contains a Rab GTPase and v-SNARE proteins which are responsible for targeting vesicles to the appropriate cellular compartment and fusion of the membranes, respectively[95]. Within the plasma membrane, there is a specific Rab effector which is recognized by the relevant Rab GTPase found within the endosome membrane and which serves in tethering the vesicle to the plasma membrane[96]. Additionally, within the plasma membrane, there is a t-SNARE protein which interacts with the v-SNARE protein embedded within the endosomal membrane[97]. All together, the binding of the Rab GTPase to the specific Rab effector within the membrane and interactions between the v-SNARE and t-SNARE proteins results in the formation of the trans SNARE complex[98]. Fusion of the two membranes commences following the hydrolysis of the GTP catalyzed by the Rab GTPase[97]. As discussed earlier, the fusion of a late endosome or MVB with the plasma membrane leads to the subsequent secretion of exosomes into the extracellular space, where they can proceed with downstream functions in recipient cells[88].

Table 1. ***Medically relevant sub-micron particles known to be secreted from cells.***

			Extracellular Vesicles		
	Retroviruses	**ERVs (Class I, II, III)**	**Exosomes**	**Microvesicles**	**Apoptotic Bodies**
Illustration	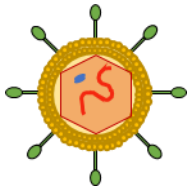	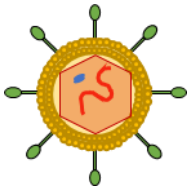			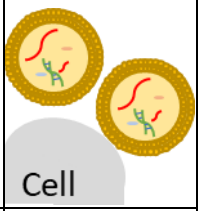
Size	≈100nm	≈100nm	<100nm (≈30-1000nm)	≈50-1000nm	≈800nm-5000nm
Egress Pathway	Budding, Exocytosis, Apoptosis	Budding, Viral Recombination	Exocytosis of MVBs (Endosomal Trafficking)	Shed from the plasma membrane	Membrane blebbing and fragmentation
Contents	RNA genome, capsid, viral enzymes, host restriction factors	RNA genome, capsid, viral enzymes	mRNA, miRNA, host proteins	DNA, mRNA, miRNA, host proteins	Host DNA, RNAs, proteins

Exosomes are released in a regulated fashion and have found to be released under stimulating conditions in which exosome secretions are upregulated or even inhibited[3,88,99]. Exosome release has been demonstrated to be increased in similar conditions to MVs such as: activation of T-cells, increased intracellular calcium levels, hypoxia, low pH, presence of extracellular ATP and more[3]. In addition to physiological increases in exosome secretions, exosomes have also been demonstrated to be upregulated under various states of pathology such as cancers, cardiovascular diseases, diabetes and more[3,8]. Previous work in cell lines demonstrated that T-cell activation using CD3 and CD28 antibodies lead to the upregulated secretion of particles sized at 103nm (exosome-size range) and 166nm[100]. Also, in addition to upregulation, some drugs and cytokines have been implicated in the inhibition of exosome release. For example, interferon I is implicated in the reduction in exosome production, through transcription and translation of the ISG15 gene, which leads to the degradation of the TSG101 protein (a subunit of the ESCRT-1 complex) involved in MVB biogenesis[90,101,102]. Drugs which block or inhibit cation transporters, like calcium channel blockers and hydrogen/potassium pumps, have also been demonstrated to inhibit exosome release by preventing increases in intracellular calcium levels, which stimulate exosome release and prevent acidification and maturation of endosomes respectively[3,99,103].

Extracellular vesicles secreted into the extracellular space, have a plethora of downstream effects on neighbouring cells or even distant tissues within multicellular organisms[104]. EVs have been the subject of extensive research to determine their

role in medicine as biomarkers of disease, pathogenicity and disease progression and as novel therapeutic strategies[3,105–108]. EVs enable intercellular communication through the donation of host-cell derived cargo and by the receptors and proteins found on their surface[109]. EVs are delivered to and received by recipient cells via fusion with the plasma membrane, endocytic pathways and binding to cell surface receptors[110,111]. The available cargoes and surface proteins vary depending on the source cell or tissues from which they are generated, their physiological state (activated, apoptotic, resting, infected, etc.), their stage of the cell cycle and, naturally, the compartments from which they originate[85,110,111]. The potentially enclosed cargoes, which are vast and many, can lead to changes in recipient cell behaviours depending on what and how much is being delivered. However, surface proteins and receptors may stimulate signal transduction pathways and increase the available receptors found on the surface of recipient cells[112].

The inherent ability of EVs to induce cellular changes in recipient cells, by directly depositing biological cargoes, has been a point of key interest in the field of EV research[107,108]. The surrounding host-derived membrane on EVs provides the cargo a sheltered environment that protects them from external degradation by degradative enzymes and which is necessary for cell-to-cell communication to function proximally or in distant tissues[113,114]. Through the transfer of biological cargoes, such as cytokines, RNAs, viral-associated products, proinflammatory and oncogenic products, cells receiving these cargoes can undergo distinct changes and may lead to the exacerbation of disease[115]. Cytokine delivery alters cellular transcription, within sensitive cells, through activation of various immune pathways

such as NF-κB and JAK-STAT signalling pathways which, in turn, lead to their own downstream and effector functions[116–118]. RNAs such as miRNAs can lead to gene silencing effects, through degradation with complimentary mRNAs, in recipient cells while transported mRNA can lead to protein translation[110,119]. Viruses, especially retroviruses, and non-enveloped viruses hijack host-cell machinery used in the transport of vesicles and release of EVs[120]. Retroviruses like HIV hijack ESCRT pathways in the process of acquiring a host cell derived envelope and subsequent release from infected cells[121]. This also results in the formation of virus-like-particles, which are EVs, that have incorporated viral-associated products but may not be replicatively competent or infectious[5,122]. Non-enveloped RNA viruses, like members of the hepatitis family of viruses, and some members of the *Totiviridae* also hijack host cell machinery and may also be incorporated into EVs; thus, enabling their dissemination, immune system evasion and exacerbation of disease[5,122–125].

In addition to the effects exerted on recipient cells by the internalization of exosome derived contents, EVs carry surface proteins which alter functions in receiving cells[126,127]. EVs have the potential to carry along many host-derived surface proteins and receptors acquired through the method of egress from the originating cell. Typical surface proteins and receptors found on EVs are the tetraspanin family of proteins, integrins and MHC I molecules[127,128]. However, the potential list of surface receptors and proteins is more vast when considering tissue specific proteins and receptors[129]. Surface proteins act as ligands which are necessary for cell attachment, while others mediate processes involved in signal transduction pathways, antigen presentation or contributing to surface cell expression upon fusion

with recipient cells[127]. ICAM1 proteins, on the surface of EVs, interact with LFA1 found on T-cells contributing to their subsequent activation[19]. Intriguingly, it has been demonstrated that EVs incorporating CXCR4 or CCR5 receptors from lymphocytes, could transfer these receptors to new tissues and thereby increase the range of susceptible tissues to HIV infection[8,19].

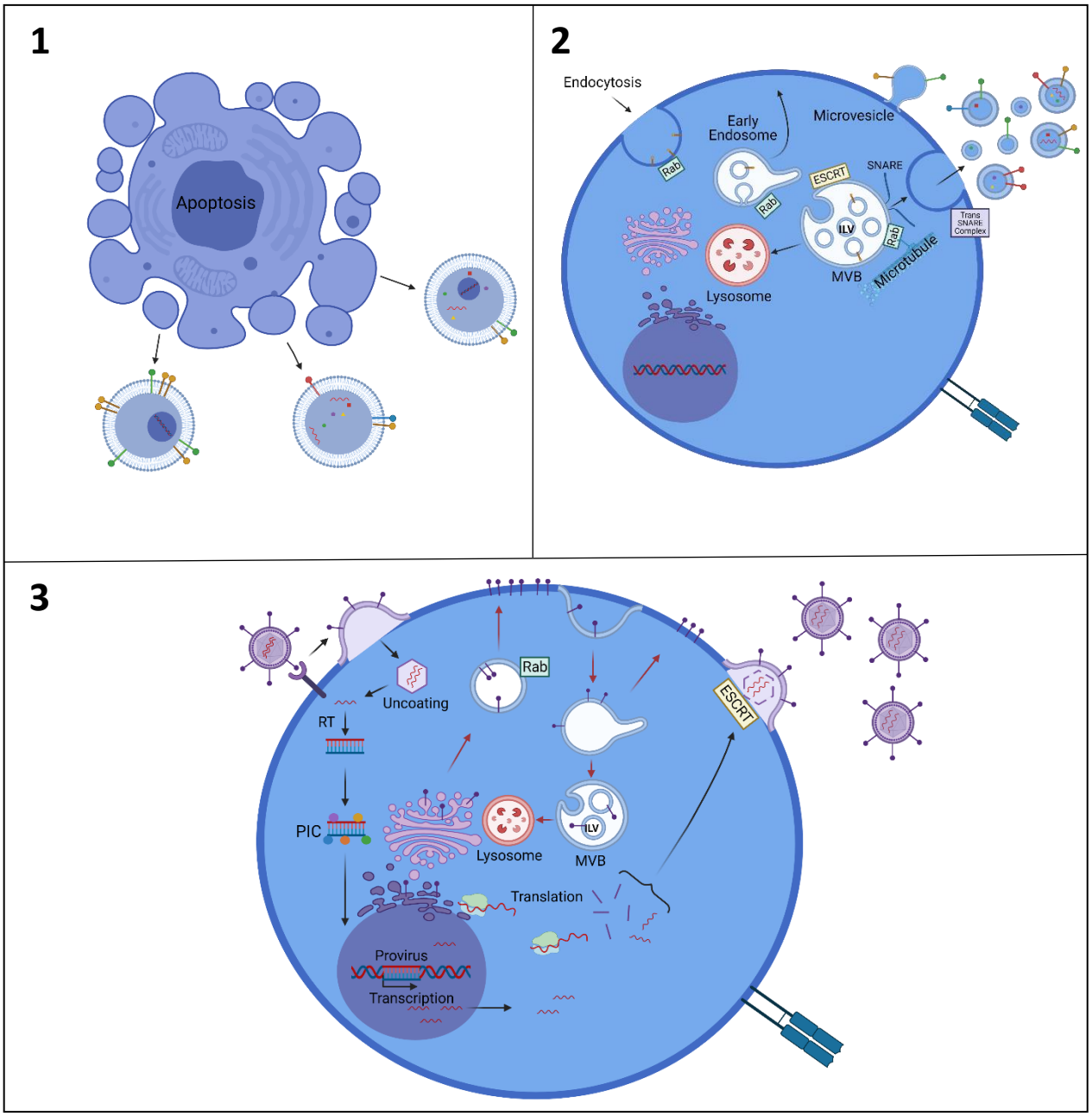

Figure 1. Particle egress pathways for EVs and Retroviruses. 1) *Apoptotic bodies bleb from the plasma membrane following the initiation of apoptosis and fragmentation of the cell and nuclear compartments.* ***2)*** *Microvesicles shed directly from the surface of the plasma membrane, preferentially at lipid raft junctions or tetraspanin enriched domains. Exosomes are intraluminal vesicles (ILV) which have been externalized to the extracellular environment following multivesicular body (MVB) fusion with the plasma membrane. MVB fusion at the plasma membrane is facilitated by microtubule filaments as well as Rab, SNARE, motor and ESCRT proteins. ILVs are generated within endocytic pathways. ILVs bud into early endosomes and MVBs. Endosomes may return to the plasma membrane or mature into late endosomes like MVBs. MVBs can fuse with lysosomes and, in doing so, release their cargo destined for degradation.* ***3)*** *Retroviruses infect susceptible cells via cell receptor binding. Infection progresses to the internalization and uncoating of the viral core where the viral genomes undergo reverse transcription (RT) forming pre-integration complexes (PIC). Pre-integration complexes are imported into the nucleus where they will facilitate the integration of the viral genomes within the host genome. Retroviruses and Endogenous retroviruses (ERV) mobilize to the extracellular environment following their transcription in the nucleus and the assembly of viral components and the RNA genomes within a viral capsid core. Retroviruses will bud from (virally encoded) glycoprotein dense regions of the plasma membrane where they acquire their envelope. Some ERVs will bud directly from the surface much like their exogenous counterparts. Less competent ERVs however may also mobilize to the extracellular environment following cellular infection by an independent exogenous retrovirus. ERVs will recombine with the invading virus and allow less mobile ERVs the opportunity to reach the extracellular space by providing the necessary vessel to reach the extracellular space. Note: Particles and cells were depicted for ease of viewing and were not developed on an accurate or proportional scale. Figures created with BioRender.com*

Methods of Microparticle & Nanoparticle Acquisition and Quantification

To be efficiently studied, methods must exist to separate cell secreted particles that are less than 1μ in diameter and free from contaminants or co-precipitating particulates not of interest. In addition, cell secreted particles must be correctly identified and quantified in some regard which can be quite difficult. Specifically, regarding invading viruses, EVs, Virus-like particles (VLPs), ERVs and newly recombinant ERVs, differentiation and characterization may prove to be exceedingly difficult due to overlap in many physical, biochemical and effector properties and functions[5,130].

Methods of Particle Isolation (Separation)

Several methods exist to isolate small particles from various source suspensions such as cell cultured supernatants and biological fluids including serum, urine, cerebrospinal fluid, and others. Common methods of particle separation are differential ultracentrifugation, ultracentrifugation using density-based gradients, size exclusion chromatography, filtration, and immunoprecipitation techniques[129].

Centrifugation remains one of the most common techniques in separating EV populations, protein precipitates and concentrating particle populations[129]. Centrifugation techniques take advantage of the disparity in density between populations of particles which comprise the secretome, enabling them to be separated and concentrated in various mediums[131]. Ultracentrifugation, as the name would suggest, is centrifugation at higher speeds than general purpose laboratory

centrifuges and ranges in speeds of 35,000rpm – 150,000rpm and generates g-forces just over 1 million x g[131]. EVs and viruses are typically sedimented from solutions between 100,000 x g and 200,000 x g[132,133]. Two centrifugation techniques typically used are differential ultracentrifugation and ultracentrifugation using density gradients which enable particle populations of interest to be separated[134,135]. Differential ultracentrifugation requires samples to be sequentially centrifuged at higher and higher speeds (or g forces) which allows sedimentation of the densest particles in a given sample progressively over time[134]. In addition to differential ultracentrifugation, researchers exploit the disparity in buoyant densities between proteins, EVs and viruses. The disparity in density between particles allow the separation and purification from precipitating proteins. This is accomplished using gradients of varying concentrations of suspensions, such as sucrose or iodixanol, during ultracentrifugation[136,137]. There are limitations with these separation strategies; specifically, the contribution of contaminating protein precipitates, disruption in EV functionality, and low input volumes, in the case of differential ultracentrifugation, which requires an additional purification step. In contrast, density-based gradients enable an enrichment and higher purity of EVs to be acquired from a sample, but result in a lower recovery of EVs from samples[129,137,138].

Size exclusion chromatography (SEC) is a method of separating EVs from contaminating proteins while maintaining their functionality; unlike, ultracentrifugation which can shear particles during sedimentation through immense centrifugal forces[138]. SEC functions by separating particles, on the basis of size, through application of a heterogeneous sample through a SEC column containing porous gel

beads of defined size[139]. Several SEC columns are available which contain beads of different sizes and the appropriate selection depends on the application. As the sample flows through the SEC column, small particles are permitted to enter the small pores, within the beads, impeding their flow rate through the column; while larger particles pass around beads and elute more readily to enable larger particles to be separated from particles of interest[140]. This enables EVs, EV subtypes, larger precipitating proteins, and lipoproteins to be separated from one another[140]. However, SEC is still unable to exclude all contaminating proteins and lipoproteins and typically results in a more dilute sample and contains a lower yield of EVs[129,141].

Filtration is a common method of separating particles and is often used, in conjunction with other purification methods, to isolate key particle populations of intrigue. Ultrafiltration is a combination of different filtration techniques all of which require removal of larger particles from a suspension, via pores or concentration gradients, which enables only small particles to traverse semipermeable pore junctions[142]. In EV and viral preparations, dead-end filtration techniques are often used such as filtering a substance through various sized membranes ranging from 0.45 microns to 0.1 microns[143,144]. Size and methods of filtration depend on the experimental setup and the populations of particles researchers seek to investigate. These techniques are paired with other purification techniques, like ultracentrifugation and SEC, to assist in clearing unwanted particulates and enhancing EV prepations[22,145,146].

Using EV specific biomarkers, antibodies can be used to bind, purify, and isolate EVs from suspensions using immunoprecipitation techniques. Commonly, general

EV markers and their antagonizing antibodies are used in immune-affinity capture techniques such as: CD9, CD63, CD81, CD82, Annexins, Alix and Rab 5 [142]. These techniques allow for highly specific isolations of EVs and EV subtypes and are adaptable to several experimental setups depending on the antibodies used. While immunoaffinity capture techniques yield some of the highest purity preparations of EVs, there are some drawbacks which make it difficult, in some instances, to assess various properties of the purified EVs. Immunoaffinity capture techniques rely on antibody recognition of EV markers. This means the quality of the isolation is dependent on the various isolation conditions and the affinities of the antibodies used[142]. As a result, samples using this technique typical results in lower recovery of EVs from suspensions[129]. Due to the immense heterogeneity in EV populations, immunoaffinity capture isolations fall short in their ability to recognize total populations[142]. Particularly, when a specific marker is not present or minimally expressed on sub populations of particles. This also contributes to the lower recovery of EVs[142]. In addition to lower recovery, antibody-based captures inhibit the functionality of EVs to be assessed post-isolation[142]. This is because it is not always possible to separate the bound antibodies from surface proteins; thereby, hindering downstream applications[142].

Table 2. *Comparison of Current Particle Separation Techniques. Yang et al. 2020 (142).*

Isolation Method	Principle	Benefits	Trade-offs
Sequential Ultracentrifugation	Particles have varying densities and sizes; enables sedimentation under sequential increasing centrifugal forces and the analysis of discrete populations over time	• Inexpensive • Low risk of co-contamination with reagents •Suitable for larger sample input volumes	• Requires a variety of equipment • Time and human resource intensive • High forces jeopardize structural integrity of precipitating particles • Co-sedimentation with proteins
Gradient Ultracentrifugation	After centrifugation in a medium of varying density, particles will remain suspended in positions of the medium with similar densities	• High purity of suspended particles • Enables sub-populations of particles to be separated	• Does not accommodate larger input volumes • Requires a variety of equipment • Time and human resource intensive • High forces jeopardize structural integrity of precipitating particles
Ultrafiltration	Filtration using a membrane with defined size-exclusion or molecular weight limits	• More efficient equipment cost • Low time cost	• Moderate purity • Comptonization of particle integrity by shear stress • Loss of separation efficiency due membrane fouling
Size-exclusion Chromatography	Particle suspensions added to porous materials enables particle separation through the elution of particles by their size, with larger particles bypassing small pores and eluting first	• High purity • Low time cost • Retains native state of eluted particles • Reproducible • Enables assessment of both small and large particles • Accommodates a variety of sample types	• Not as cost effective • Requires prior particle concentration or enrichment before processing
Immunoaffinity Capture	Based on specific binding affinities between particle surface markers and immobilized antibodies	• Enables sub-populations of particles to be separated • High-purity preparations • Not technically challenging • Low risk of reagent contamination	• Requires a variety of antibodies and optimization • Does not accommodate larger input volumes • Requires prior particle concentration or enrichment

Methods of Particle Acquisition and Quantification Techniques

Extracellular vesicles and viruses are sub-micron structures which make them more difficult to identify and analyze. Researchers have developed several methods in order to visualize, identify, quantify and enumerate the various key constituents which make up the cellular secretome. Some examples include, flow cytometric based techniques, proteomic analyses, microscopy techniques and more biophysical based acquisition methods[147]. The methods used to purify and/or concentrate sample preparations will greatly influence the suitability of one technique over another. Typically, more than one technique is imperative to provide a well-rounded interpretation of the particles analyzed and answer specific research questions.

Flow cytometry is a high-throughput method that has been used to analyze populations of cells and viruses over the last few decades[148]. Conventionally, flow cytometers are useful for identifying cells and larger structures[149]. However, they lack the sensitivity necessary to efficiently resolve nanoparticles from instrumental background noise; as such, more sensitive cytometers and techniques were developed to analyze nanoparticles more effectively[150]. Nanoscale Flow Cytometry (NFC) was developed with the goal of resolving nanosized structures from background signals and being able to overcome the limits of detection on conventional flow cytometers for this purpose[22,149,150]. NFC describes methods of flow cytometry which have been carefully fine tuned and optimized with the deliberate purpose of analyzing sub-micron particles like extracellular vesicles and viruses[22]. These methods make use of light scattering to enable large heterogenous populations of particles to be differentiated from background signals or contaminants

and identify selective subsets of particles, using fluorescent labelling techniques, under many distinct parameters[150,151]. In addition, NFC enables the number of particles per volume in a sample to be determined, as well as the size of particles when combined with size reference microspheres[145,151,152].

Resistive pulse Sensing (RPS) and Tunable Resistive Pulse Sensing (TRPS) are high-throughput and efficacious ways of quantifying size, concentration, and charge of particles in a sample by monitoring disruptions in electrical current or electric impedance as individual particles pass successively through a nanopore[153].

Nanoparticle Tracking Analysis (NTA) is a bulk analysis method which validates the size distribution of particles in suspension, while also providing images and videos of particles ranging from 10-1000nm[154,155]. NTA instruments are comprised of a laser which passes through a sample cell channel where the light is refracted or scattered by particles in suspension and focused through a microscope[156]. A digital camera records the light scatter and computer software tracks individual particles and correlates their Brownian motion, directly with their size, while also providing video footage of recorded particles[156]. In addition, NTA instruments are capable of measuring the Zeta potential, or electrical charge on the surface of particles in suspension, through the application of an electric field across the cell channel and measuring the velocity of particles towards the oppositely charged electrode[157]. However, one setback is the NTA, as mentioned previously, is a bulk analysis method of analyzing particles in suspension and therefore is unable to differentiate particles of overlapping size/Brownian motion (i.e. a 200nm virus from a 200nm

EV)[145]. This demonstrates the importance of purification methods and isolation techniques to provide more reliable data.

Transmission electron microscopy (TEM) allows individual particles such as viruses and EVs to be analyzed and provide insight into size, morphology, and purity of a sample[158]. As opposed to light scattering microscopes, electron microscopes use a beam of electrons which travel through the sample and magnify the images[159]. TEM enables incredibly high-resolution images to be viewed[159]. While TEM is critical to identify and characterize the type of particles in a sample, it is lacking in its ability to analyze a large number of particles in a sample efficiently, in contrast to more bulk or high-throughput techniques[129].

The above-mentioned techniques provide different strengths for the quantification and characterization of particle populations in a given sample; but a combination of analytic techniques is more robust and enables the limitations of individual techniques to be overcome.

The field of extracellular vesicle research is vast and continues to rapidly expand. Much effort has been dedicated to understanding the roles ERVs and EVs play in a plethora of pathological conditions and as a therapeutic strategy acting as a vector for drug delivery[3,8]. The exact mechanisms and coordinated efforts of EVs, with additional regulatory pathways, adds a potential multi factorial combination with other biological systems and pathways which complicate clear/precise understanding of the role these particles play in regular physiology, pathological conditions, and drug treatment[160]. As such, a thorough understanding of EV behaviour, physiology and the “puppet-master” pathways, which modulate their

secretion, is essential before their role(s) can be defined under abnormal conditions. Particularly helpful studies on the role EVs play in host immune systems is crucial as the host immune system is at the critical junction between healthy physiology and states of pathology and disease. Obstruction, disruption, misemployment, and inhibition of these pathways, potentially by EVs, and systems is likely to lead towards sickness and disease. Extracellular vesicles and endogenous retroviruses may play important immunomodulatory roles and/or may lead to exaggerated or exacerbated conditions of disease. Extracellular vesicles act as an intercellular delivery system that all cell types use. Hijacking or improper regulation of these pathways, such as in states of disease, exacerbates and complicates clear mechanisms of actions and hinders the immune system's ability to effectively suppress and remove foreign entities. As well, even though this is highly relevant and important, it complicates our understanding of EV behaviour and EV physiology which makes EV pathology difficult to study. Here, we demonstrate preliminary work which begins to characterize the particles and particle subsets secreted by primary murine naïve $CD4^+$ T-cells, under distinct stimulatory conditions, by nanoscale flow cytometry and nanoparticle tracking analysis to further our collective understanding of EV physiology and behaviour.

Study Aims, Objectives and Hypotheses

Aims

Relate patterns of EV release and key secretory pathways by murine naïve $CD4^+$ T-cells with immunologically relevant stimuli.

Objectives

Develop the necessary conditions to optimally stimulate murine naïve $CD4^+$ T-cells.

Collect, characterize, and quantify secreted particles by flow virometry and nanoparticle tracking analysis.

Hypothesis

Under distinct immune stimulating conditions, murine naïve CD4+ T-cells will secrete various particles in distinctive egress profiles. This will enable the characterized profiles of particles to be correlated with specific stimulated immune pathways.

Goal

Ultimately, be able to identify and relate similar patterns of EV subsets and EV release, with pathological conditions in humans, and use this as a rapid and efficient diagnostic tool.

Materials & Methodology

Establishing conditions to optimally stimulate murine Naïve CD4+ T-cells

Murine Naïve $CD4^+$ T-cells were acquired from the spleens of C57BL/6 N female mice aged eight weeks. Mice were ordered from Charles River Laboratories and housed in the main animal care facilities provided by the University of Ottawa at Roger Guindon Hall.

Mice were euthanized using CO_2 and cervical dislocation, in compliance with Animal Care and Veterinary Services guidelines at the University of Ottawa, and in accordance with the Canadian Council on Animal Care guidelines. Spleens were carefully extracted from three separate mice matched by sex. Spleens were collected and stored in cold PBS, containing one percent FBS, and placed on ice until splenocytes were further purified.

In a biological cabinet, splenocytes were purified and harvested from homogenized mouse spleens. Following purification, naïve $CD4^+$ T-cells were isolated using a $CD4^+$ Naïve T-cell Isolation Kit provided by Miltenyi Biotec which separates cells through magnetic negative selection. Naïve $CD4^+$ T-cells were subsequently plated on pre-coated 48-well plates containing CD3 and CD28 antibodies at a seeding density of $2.0x10^6$c/mL. This activation of naïve $CD4^+$ T-cells ensured adequate cell viability and proliferation required for the duration of the experiment. Cells were incubated for a minimum of 48 hours at 37°C with 5% CO_2 to achieve necessary cell densities required for the number of treatment groups and conditions.

Following naïve $CD4^+$ T-cell culturing, cells were harvested, counted using a Bio Rad TC20 cell counter, split and resuspended in media supplemented with “EV-depleted” FBS and desired immune and pharmacological stimulants to simulate relevant medical and biological conditions such as: Phorbol-Myristate-Acetate (PMA) with Ionomycin (PMA/I). Each treatment required titration of the desired stimulant to maximize immune activation and particle egress while maintaining cell viability. For PMA treatments, PMA concentrations of 5, 10, 25 and 50ng/mL were assessed while maintaining a concentration of ionomycin at 1µM across all drug treatments. In addition to drug treatment, culturing media RPMI was supplemented with $CaCl_2$ to a final concentration of 1.5mM in order to assist with the degrees of activation[161].

Following cell activation, cells and supernatants were harvested and separated by centrifugation at 900g for 10 minutes. Supernatants were removed and 0.45µ syringe-filtered using VWR Acrodisc® Syringe filters (#CA28143-352) to remove cells or large cellular debris from suspended particles of interest. Cells were resuspended in PBS and centrifuged at 500g for 10 minutes; this step was repeated two additional times to prepare cells for staining and labelling. Cell concentrations were counted by the Bio Rad TC20 Cell Counter. Cells from treatment groups viability and levels of activation was assessed, using a Fixable Viability Stain 450 provided by BD Biosciences (#562247) and a PE fluorescently conjugated CD69 antibody from BioLegend (#104507). Cells, with the exception of non-stained controls, were stained with viability stain at room temperature for 15 minutes (away from light). Cells were washed with PBS three times and subsequently stained with CD69 antibodies at a final concentration of 0.25µg/mL per $1.0x10^6$ cells at 4°C for 20

minutes. Cells were once again washed three times with PBS to remove unbound antibodies. Cells were analyzed on the BD FACSCelesta™ flow cytometer. It was essential to monitor the health and activated nature of cells, within treatment groups, as these parameters will directly affect the quantity and types of particles being released. Optimization of stimulatory conditions was, therefore, necessary in order to more precisely correlate particle egress with cell stimulants and maintain egress profiles between replicate experiments.

Nanoparticle Tracking Analysis using Particle Metrix Zeta View®

Allocated supernatants were diluted 1:40 with 0.1µ syringe-filtered D-PBS (#311-425-CL) to a total volume of 2mL. Samples were siphoned into 1mL syringes compatible with the Zeta View system. The Zeta View was flushed with 10mL of sterilized Mili-Q water and calibrated and focused using counting beads. The fluidics were flushed again with sterilized Mili-Q water until no counting beds were observable in any camera position. The fluidics were primed with 0.1µ syringe-filtered D-PBS before samples were loaded. Samples were then acquired one at a time with a 0.1µ syringe-filtered D-PBS rinsing step in between. Analysis of particle suspensions by NTA enabled the concentration of total particles, within treatment groups, to be determined and compared to controls and other treatment groups. In addition to original total particle concentration, NTA enabled distinct particles to be categorized by size, enabling smaller particles like exosomes to be identified and differentiated from larger particles like microvesicles.

Nanoscale Flow Cytometry using the Beckman Coulter CytoFLEX Flow Cytometer

By staining and labelling particle suspensions with dyes and fluorescently conjugated antibodies, the type and abundance of particles was further dissociated from the heterogenous population of particles. Samples were further split in order to selectively stain and label populations of interest like extracellular vesicles and endogenous retroviruses within the same sample.

Samples were stained with carboxyfluorescein succinimidyl ester (CFSE), one type of dye which has been used to stain extracellular vesicles, at a final concentration of 0.5µM in a total volume of 200µL. The use of fluorescent antibodies conjugated to known exosomes markers enabled more specific particle differentiation. Tetraspanin antibodies CD9 and CD81 provided by Biolegend (#124805 #104905) were used at a final concentration of 1.6µg/mL to enable exosome populations to be identified[129]. Both antibodies were added to CFSE stained tubes and non-CFSE stained controls at final concentrations of 2µg/mL. All samples were incubated at 37°C for one hour. Following staining, all samples were diluted 1:100 with 0.1µ syringe-filtered D-PBS to a total of 1mL. The Cytoflex instrument was cleaned for 15 minutes and rinsed with sterile Mili-Q water for an additional 15 minutes before use. Samples were run one at a time and the fluidics were rinsed with sterile Mili-Q water in between each sample.

Methods of Data & Statistical Analysis

Assessing Statistical Significance for PMA Titration Experiment

Data acquired from nanoparticle tracking analysis was used to assess statistical significance via Welch's T-test and Welch's ANOVA Test where applicable using GraphPad Prism 8 Software. Each T-cell PMA treatment group (PMA 5, 10 & 25ng/mL) was compared to both DMSO and RPMI T-cell groups for statistical significance by Welch's T-test. The varying dosages of PMA T-cell treatments were assessed for statistical significance by Welch's ANOVA test. In all cases, normality was assumed following the central limit theorem as all supernatants contained greater than 30 particles per sample (i.e. n=30<). A Games-Howell post hoc multiple comparisons test was additionally performed, post ANOVA testing, to avoid bias and assess the combinatorial impact of one-way ANOVA testing between treatment groups. This enabled the effect of PMA dosage on secreted particle size to be determined. This experiment was not performed in replicate.

Assessing Statistical Significance for PMA Time Course

Similar methods to the previous experiment were performed to assess statistical significance between distinct treatment groups using GraphPad Prism 8 Software. Again, normality of each distribution was assumed as the number of particles per sample was well above n=30 following the Central Limit Theorem. Treatments from the 12-hour incubation period were grouped together and the 24-hour incubation

treatments were grouped separately. Analysis of both the 12- and 24-hour treatments involved statistical analysis using the Welch's T-test between the PMA treated group and the RPMI and DMSO groups individually. As, in this experiment, the concentration of PMA was fixed, no ANOVA test was performed. Instead, the 12- and 24-hour PMA treated groups were compared using a Welch's T-test to determine statistical significance between incubation period and particle size. This experiment was not performed in replicate.

Gating strategies, Controls and Software Analyses for PMA Titration & Time Course

By using flow cytometry, cells' viability and surface expression of CD69 was able to be monitored to assess the degree of T-cell activation by PMA while ensuring cell viability was not jeopardized. In FlowJo software cells were gated on by isolating single cell populations by FSC-A vs. FSC-H channels and then analyzing gated cells within the fluorescent BV421-H and FITC-H channels. A quadrant gate was set relative to the unstained control and the positively stained sample, to discriminate between positively and negatively stained cells for both channels.

By NFC, supernatants were split and stained with CFSE dye as well as CD81 and CD9 fluorescently conjugated antibodies or combinations of CFSE and one of the mentioned antibodies. Controls consisted of preparations of PBS and the culturing media used. For each given sample and controls there was an unstained control, CFSE stained, CFSE + CD81 and CFSE + CD9 samples. The PBS samples controlled for background noise of the Cytoflex and unspecific fluorescence, produced by either the CFSE, CD81 or CD9 antibodies. The culturing media samples controlled for background instrument noise or interactions with signals

provided by the culturing media and any shifts in fluorescence due to staining the culturing media. The culturing media also served as an isotype control for unspecific fluorescence, resulting from the fluorescently conjugated antibodies. As the antibodies used were Rat monoclonal antibodies and were not demonstrated to cross-react with CD81 on bovine EVs (acquiring from the FBS supplemented within the culturing media), the media served as an appropriate isotype control. To ascertain the MFI produced within successfully stained populations samples were gated on as follows. First, the background signal which appears high in the VSSC-H channel was gated out. Next, the population was analyzed by VSSC-H versus the relevant staining channel (FITC-H for CFSE, PE-H for CD81 and CD9). A rectangular gate was created above the background signal (positive on the PE or FITC axes) representing positively stained particles. For a given sample the gate was created relative to both the unstained and stained controls, enabling successfully stained particles to be identified. The mean fluorescent intensity and standard deviation was calculated for all particles found within the positively labelled gates by FlowJo software. MFI produced within the background media control was removed from samples MFI. This enabled fluorescence solely produced by the labelling of particles within treated samples to be quantified. Differences between samples MFI was assessed by Welsch's ANOVA and Welsch's T-test.

Results

Optimization of PMA/I Activating Conditions in Naïve $CD4^+$ T-cells

To begin characterizing and quantifying particle secretions under distinct immune stimulating conditions, we first attempted to simulate T-cell activating conditions using PMA and Ionomycin. To mimic activating conditions, the dosage of PMA necessary to activate T-cells sufficiently, needed to be determined. PMA activates protein kinase signalling pathways promoting transcription without the need of T-cell receptor binding. Both the concentration and incubation length of PMA/I applied to Naïve T-cells required investigation before secreted particle populations could be assessed to ensure representative data collection. The optimal dosage and incubation period of PMA and Ionomycin needed to achieve maximal particle output while very minimally jeopardizing cell viability. Dosage was assessed first in primary $CD4^+$ mouse T-cells extracted and isolated from the spleens of 3 separate female C57BL6/N mice. Naïve $CD4^+$ T-cells were isolated using the Milentyi Biotec kit and the purity of the isolation was assessed by flow cytometry using viability staining as well as CD3, CD4 and CD62L selective antibodies (Figure 2) Naïve T-cells were activated under conditions of 5, 10 and 25ng/mL of PMA including 1µM Ionomycin for each condition containing PMA for 12-hours at 37°C.

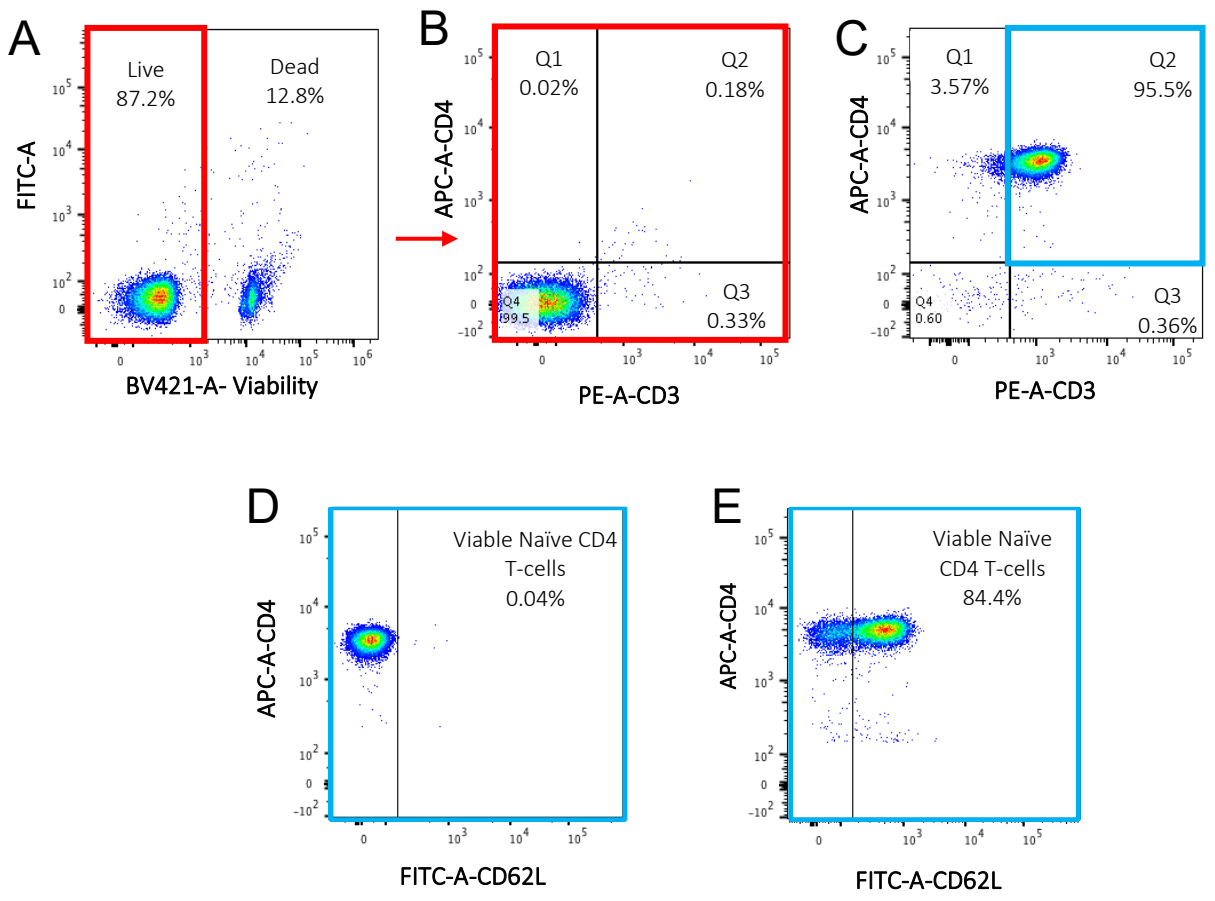

Figure 2. Purity Assessment of Naïve CD4⁺ T-cell Preparations using Miltenyi Biotec's Naïve CD4⁺ T-cell Isolation Kit. *Homogenized mouse spleens were purified and isolated for Naïve CD4⁺ T-cells via magnetic separation using an isolation kit.* ***A)*** *Post-isolation, cells were stained with viability dye. The live population (negatively stained population) was gated on.* ***B)*** *Cells stained with viability dye post-gating not stained with labelling antibodies.* ***C)*** *Cells stained with viability dye, CD3 (PE) and CD4 (APC) antibodies following Live/Dead gating.* ***D)*** *Following gating in part C, CD3 and CD4 positive cells were further gated on.* ***E)*** *Cells stained with viability dye, CD3, CD4 and CD62L antibodies. Demonstration of the percentage of CD4⁺ and CD62L⁺ (FITC) cells, following magnetic bead separation, using the isolation kit.*

Post-activation, cell viability and levels of activation were assessed and monitored by cell staining and surface expression of CD69 (Figure 3). Flow cytometry unveiled that PMA treatments reported lower percentages of cell death than non-activated treatments and T-cells treated with 25ng/mL PMA reported the highest CD69 expression compared to other PMA treatment groups. NFC analysis of activated supernatants stained with CFSE demonstrated that the percentage of EV contribution to the total number of events increased with PMA treatment (Figure 4). Staining the supernatants with CFSE, and either exosome marker CD81 or CD9, demonstrated a similar pattern in increased presence with increasing PMA treatment. However, very few CFSE positive and exosome marker positive subsets were observed (Figures 5 & 6). The differences in PMA dosage yielded significant differences in the number of particles susceptible to CFSE staining (Figures 5, 6, & 7). Nanoparticle tracking analysis demonstrated an increase in particle concentration within supernatants harvested compared to non-PMA treated samples, suggesting an increased frequency of smaller particles in treated samples (Figures 8 & 9). Treating the T-cells with 25ng/mL PMA and 1µM Ionomycin for 12 hours at 37°C, provided the largest output of particles and reported the least cell death across treatments (Figures 3 & 8).

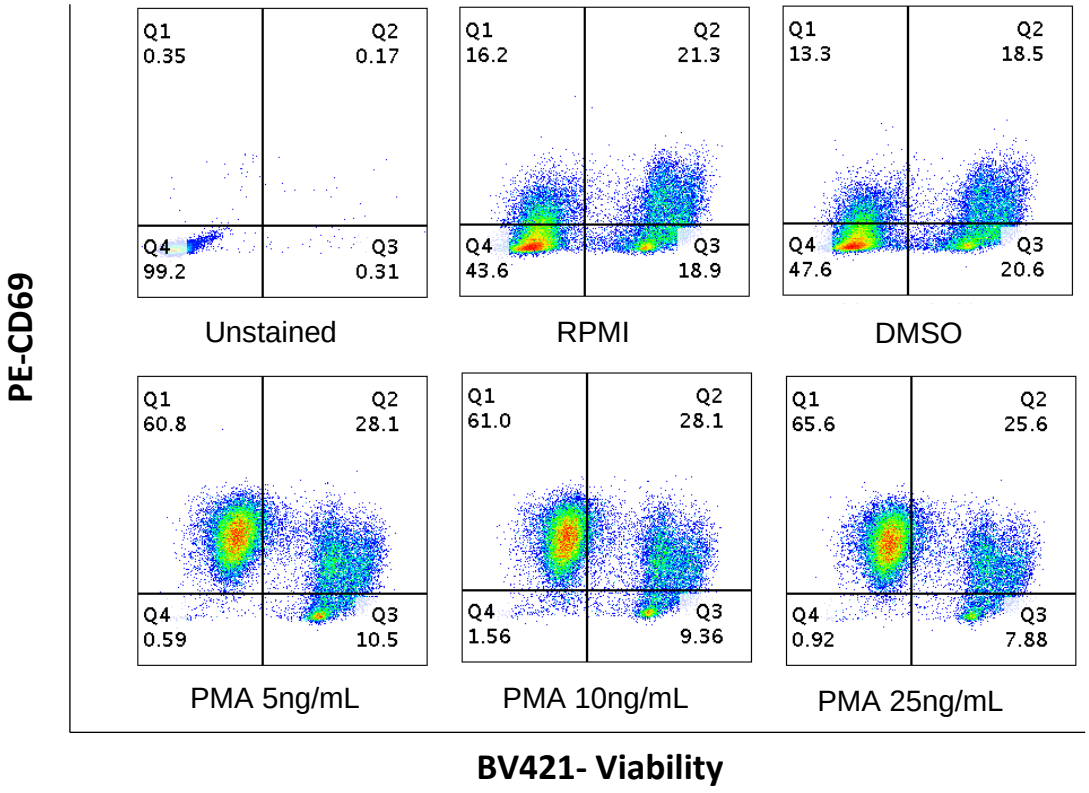

Figure 3. Naïve CD4⁺ T-cells Post-Activation Treated with PMA/I. *Following activation, the health and level of activation of T-cells was monitored by cell staining with viability dye and CD69 surface labelling and analyzed by flow cytometry. Comparing the groups activated with PMA/I (bottom row) with the non-treated Naïve T-cells (Top middle) and the Naïve T-cells treated with media and equal dosage of DMSO (Top right), there is an apparent shift in the presence of CD69 on the surface of cells. The Naïve T-cells treated with 25ng/ml PMA reported the highest labelling with the CD69 antibody and the highest viability across all treatments.*

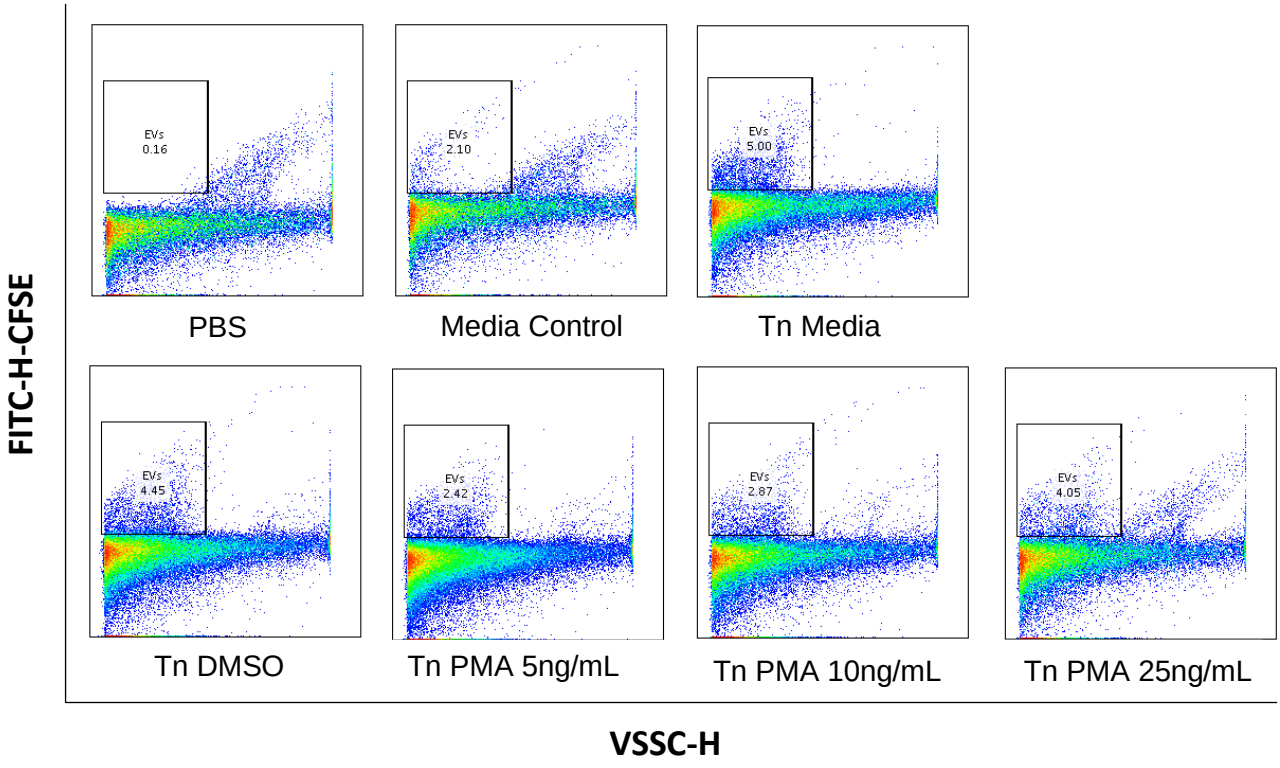

Figure 4. T-cell Supernatants Post-Activation (Stained with CFSE) NFC. *The PBS (Top Left) stained with CFSE provides insight into the background provided by the cytometer as well as the contribution of the CFSE to the background signal. Comparing the media control (Top Middle) to the PBS control there is a positive shift in the FITC channel when CFSE is added and EVs are detectable. Supernatants harvested from Naïve T-cells are denoted with "Tn". Naïve T-cells treated with PMA/I (Bottom Row) present increasing EV contribution with increasing dosages.*

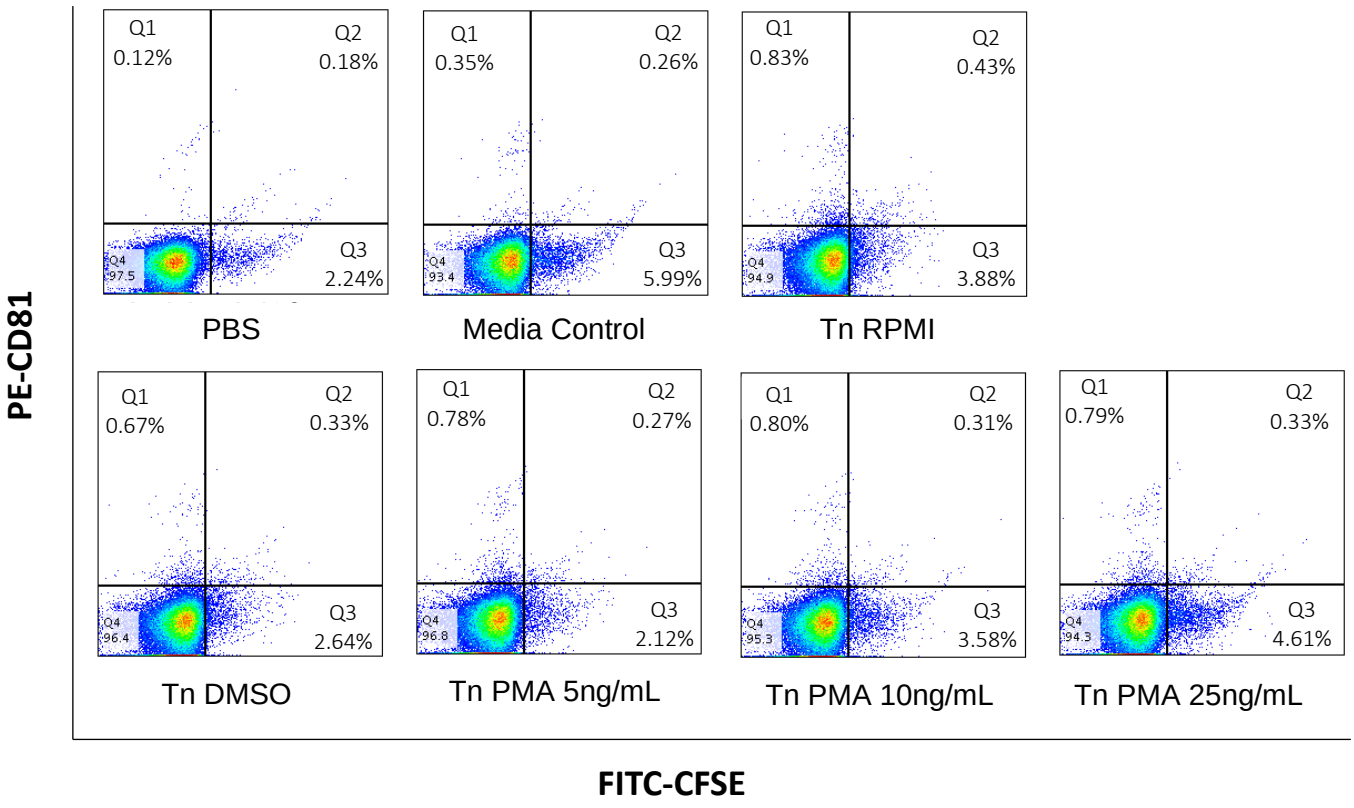

Figure 5. T-cell Supernatants Labelled with CFSE and CD81 exosome specific marker. *In the PMA treated groups, the percentage of CFSE positive particles increases with dosage but minimal differences in the percentage of CD81 and double positive particles are observed. Supernatants harvested from Naïve T-cells are denoted with "Tn". The stained media control (Top Middle) reported fewer total events than cell treated groups but still demonstrates positive CFSE and CD81 labelling due to the FBS. The PBS control (Top Left) demonstrates significant background signal provided by the antibody and CFSE dye.*

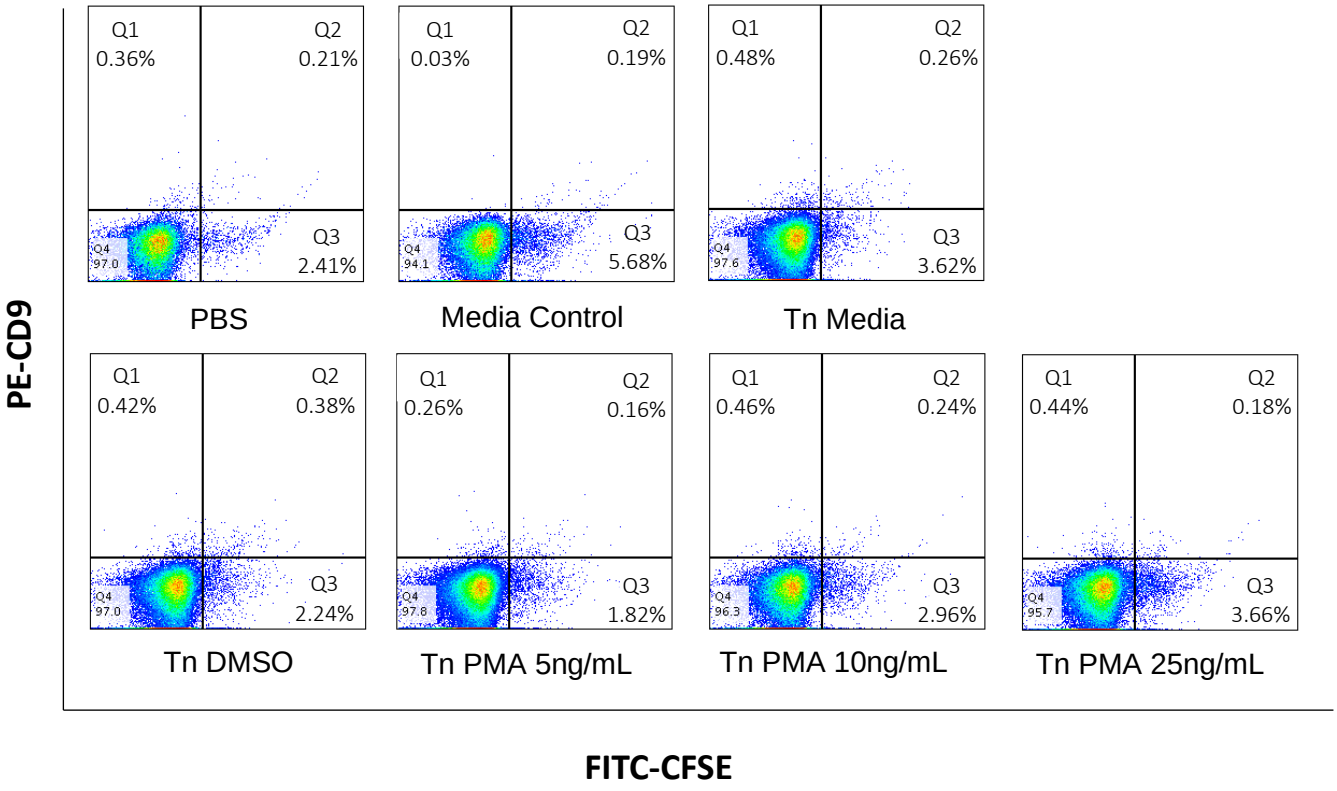

Figure 6. T-cell Supernatants labeled with CFSE and CD9 exosome specific marker. *In the PMA treated groups, the percentage of CFSE-positive particles increases with dosage but minimal differences in the percentage of CD9 and double positive particles are observed. Supernatants harvested from Naïve T-cells are denoted with "Tn". The stained media control (Top Middle) reported fewer total events than cell treated groups but demonstrates a high percentage of positive CFSE particles from the FBS and few CD9 particles. The PBS control (Top Left) demonstrates significant background signal provided by the antibody and CFSE dye.*

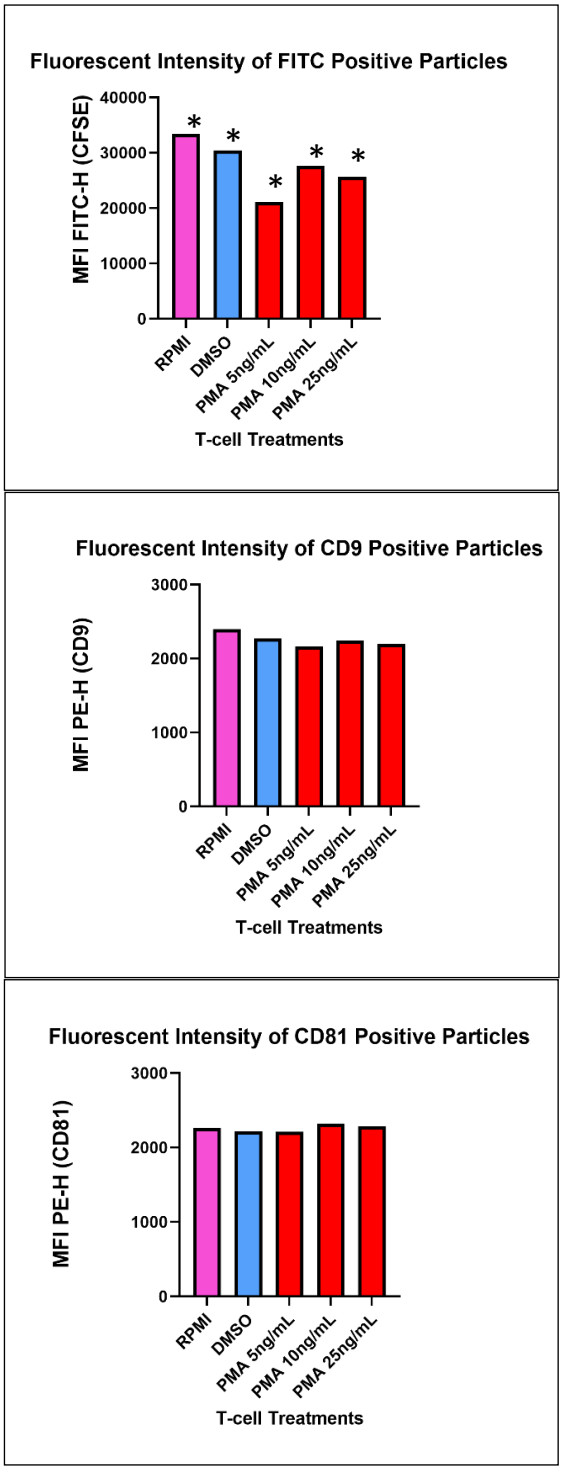

Figure 7. Analysis of Mean Fluorescent Intensities of Positively Labelled Secreted for Various T-cell Treatments. *Particles secreted from treated T-cells were stained with CFSE and CD81 or CD9 fluorescent antibodies. The various T-cell treatments are listed on the x-axis. RPMI represents T-cells cultured in RPMI media containing "EV-depleted" FBS, DMSO represents T-cells treated in RPMI media containing "EV-depleted" FBS and a comparable concentration of DMSO to the highest PMA/I treated T-cells (25ng/mL). Mean fluorescent intensity for the respective channel for each labelling method is listed on the y-axis. Positively labelled particles, as compared to controls, were gated on and the levels of fluorescent intensities assessed by FlowJo Software. One-way ANOVA analyses (and their permutations) were performed for all treatments, statistical significance is denoted by an asterisk representing an obtained P value <0.0001. Experiment was not performed in replicate (n=1).* ***A)*** *One-way Brown's-Forsythe & Welch's ANOVA analyses on CFSE-positive particles secreted under varying titrations of PMA/I was performed. Treatments mean fluorescent intensities in the FITC-H channel were found to be significant P <0.0001.* ***B)*** *One-way Browns-Forsythe & Welch's ANOVA analyses on CD9-positive secreted particles were performed. Mean fluorescent intensities across all treatments did not demonstrate statistical significance.* ***C)*** *One-way ANOVA analyses on CD81-positive secreted particles were performed. Treatments were not found to be significantly different.*

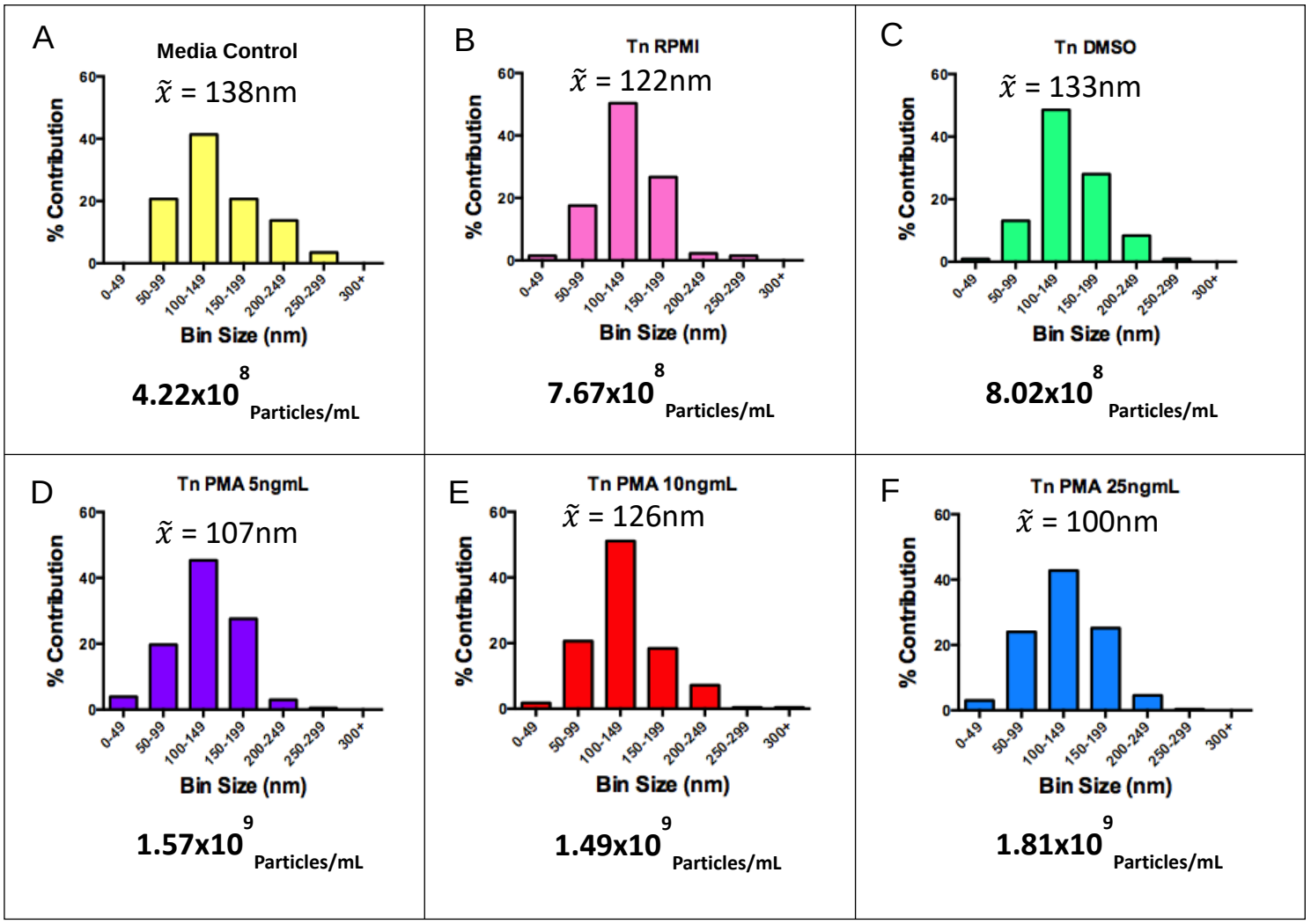

Figure 8. T-cell Supernatants Quantified by Nanoparticle Tracking Analysis. *Particle size distributions, median particle size and total particle concentration, per treatment group, are listed here. Where x-tilde represents the median particle size in a given sample and the particle concentration listed includes the dilution factor of the sample run on the instrument. Supernatants harvested from Naïve T-cells are denoted with "Tn". A) Contribution of particles provided by growth media only. B) Supernatant from untreated Naïve T-cells left in growth media only. C) Supernatant from untreated Naïve T-cells with the same concentration of DMSO as would be found in PMA treated groups. D) Supernatant from Naïve T-cells activated with 5ng/mL PMA and 1μM ionomycin. A difference in particle count is observed as well as a disparity in median particle size compared to untreated controls. E) Supernatant from Naïve T-cells activated with 10ng/mL PMA and 1μM ionomycin. No significant increase in particle count is observed compared to the 5ng/mL PMA treated group but an apparent shift in median particle size is observed. F) Supernatant from Naïve T-cells activated with 25ng/mL PMA and 1μM ionomycin. Reported the highest number of particles and the largest negative shift in median particle size when compared to untreated groups. All PMA treatment groups were found to be significant when compared to both RPMI and DMSO control groups by Welch's T-test ($p<0.0001$). All PMA treatment groups were found to be significant by Welch's ANOVA ($p<0.0001$) and by Games-Howell's multiple comparison test ($p<0.0001$). This experiment was not performed in replicate ($n=1$).*

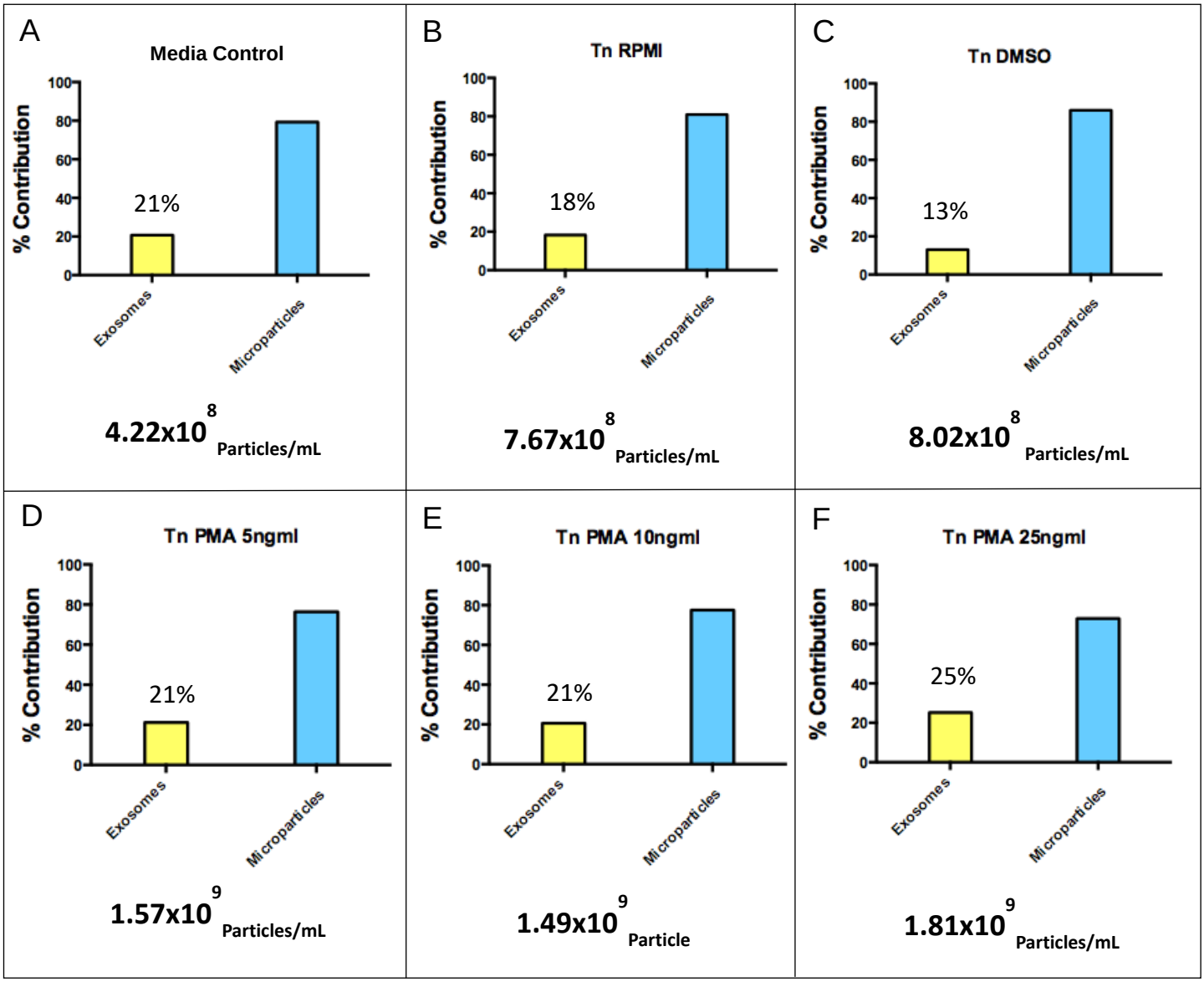

Figure 9. T-cell Supernatants Sorted by Particle Type by Size. *Treatment groups sorted by biological particle size. Exosomes were defined by particles ranging from 40-100nm in size while microparticles were defined as particles ranging from 100nm-1000nm. There is an increase in exosome-sized particles in PMA treated groups (D, E, F) when compared to untreated controls in B and C. Supernatants from Naïve T-cells activated with 25ng/mL PMA and 1μM ionomycin displayed the highest percentage of exosome-sized particles compared to other PMA treatment groups.*

Following the assessment of PMA concentration, the length of activation was assessed. The concentration of PMA was fixed at 10ng/mL across each time point. Activations were monitored at 0, 12 and 24 hours of activation or treatment. Naïve T-cell viability was 91% assessed at time point 0 by trypan blue staining and counted using a hemocytometer by the TC20 cell counter. Viability and level of activation, at 12- and 24-hour time points, were assessed by cell staining and surface labelling with a CD69 antibody conjugated to PE. It is clear, between the 12- and 24-hour time points, that there was a decrease in viability and that cell death increased with prolonged PMA/I incubation (Figure. 10). The supernatants from treatment groups were then analyzed by NFC for zero, twelve and twenty-four-timepoints (Figures 11 through 15). The 0-hour timepoint sample controls for stimulated particle release as a result of application of the suspension to the cells. CFSE was used to label particles, alongside conjugated antibodies, against EV makers (CD9-PE and CD81-PE) in an attempt to pull out population subsets of interest from the total. CFSE and CFSE-antibody combined labelling techniques proved to be successful in labelling particle subsets. By NFC, 24-hour treatments reported higher numbers of CFSE, CD9 and CD81 positive particles compared to 12-hour treatments apart from the DMSO treatment labelled with CFSE and CD81-PE. By NFC there was significant difference in fluorescence intensity produced by labelled supernatants harvested at 12- and 24-hour timepoints (Figure 16). In addition to NFC, supernatants were analyzed by NTA (Figures 17 & 18).

Overall, the effect of increased incubation period resulted in higher concentrations of released particles as well as a decrease in median particle size.

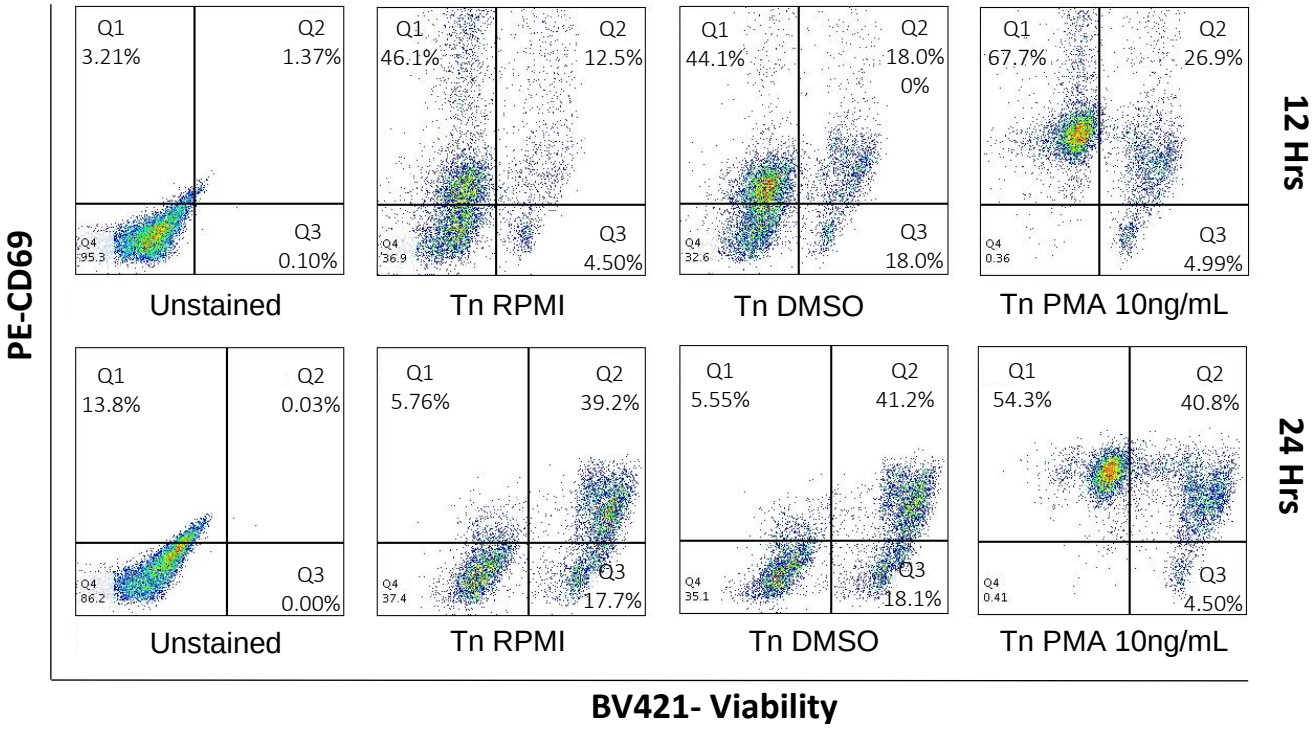

Figure 10. Viability of T-cells at 12- and 24-hour time points post activation. *Cells' viability was assessed by viability dye staining and activation was monitored via labelling with a CD69 specific antibody. T-cells incubated with PMA/I for 12 hours (Top Row) reported higher levels of viability than those cultured for 24 hours (Bottom Row). Treatment with PMA led to a positive shift in the PE channel indicating a greater surface expression of CD69 in treated groups compared to non-PMA-treated groups.*

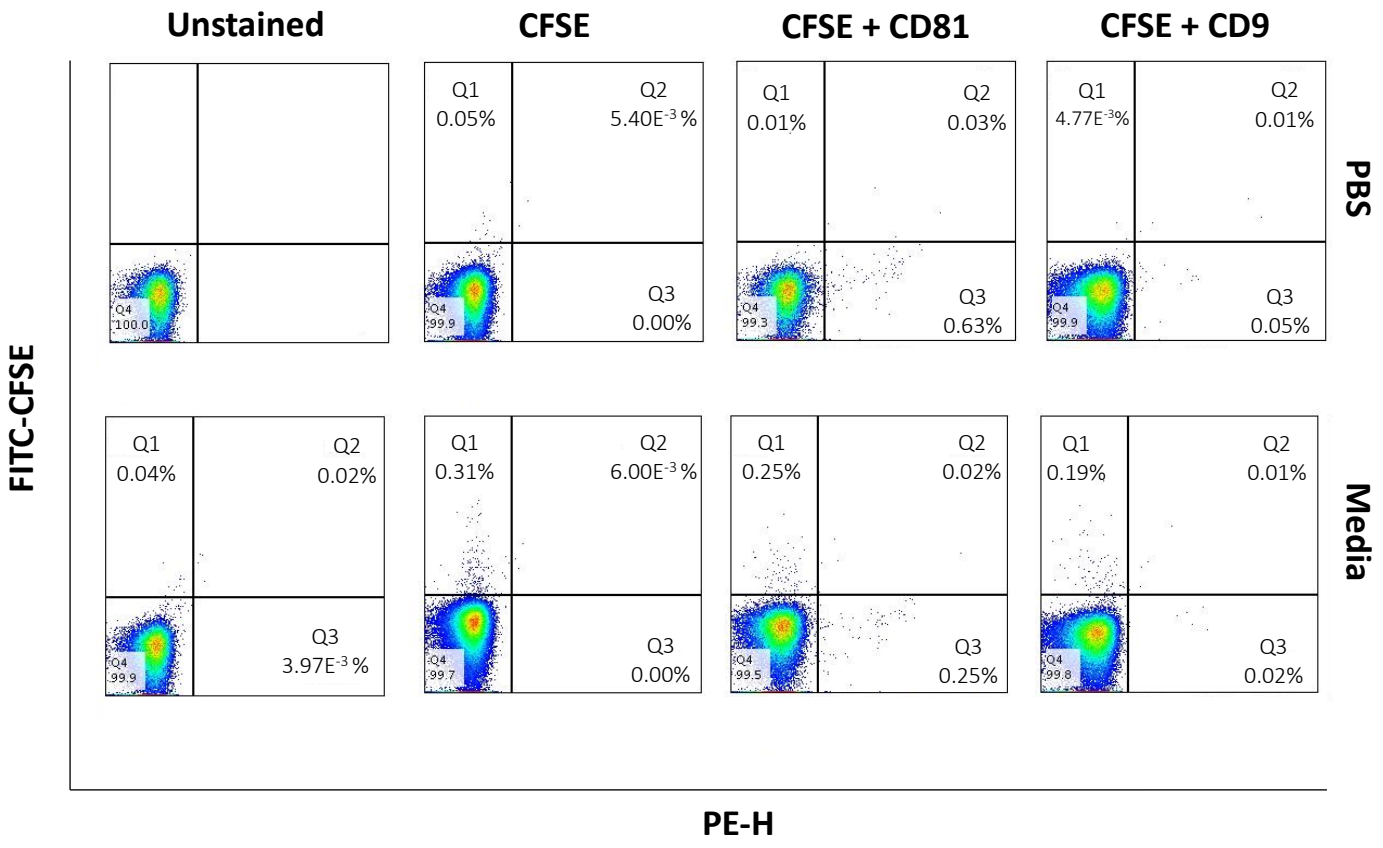

Figure 11. NFC Controls for supernatants harvest at 0- and 12-hour time points. *The top row consists of PBS controls, with and without individual and dual staining, representing the background provided by the instrument under these specific conditions. The bottom row consists of culturing media controls, with and without individual and dual staining, representing the apparent background provided by the staining in these conditions. Dual stainings with CFSE and either CD81 or CD9 provided very minimal background signals in PBS and in the culturing media used.*

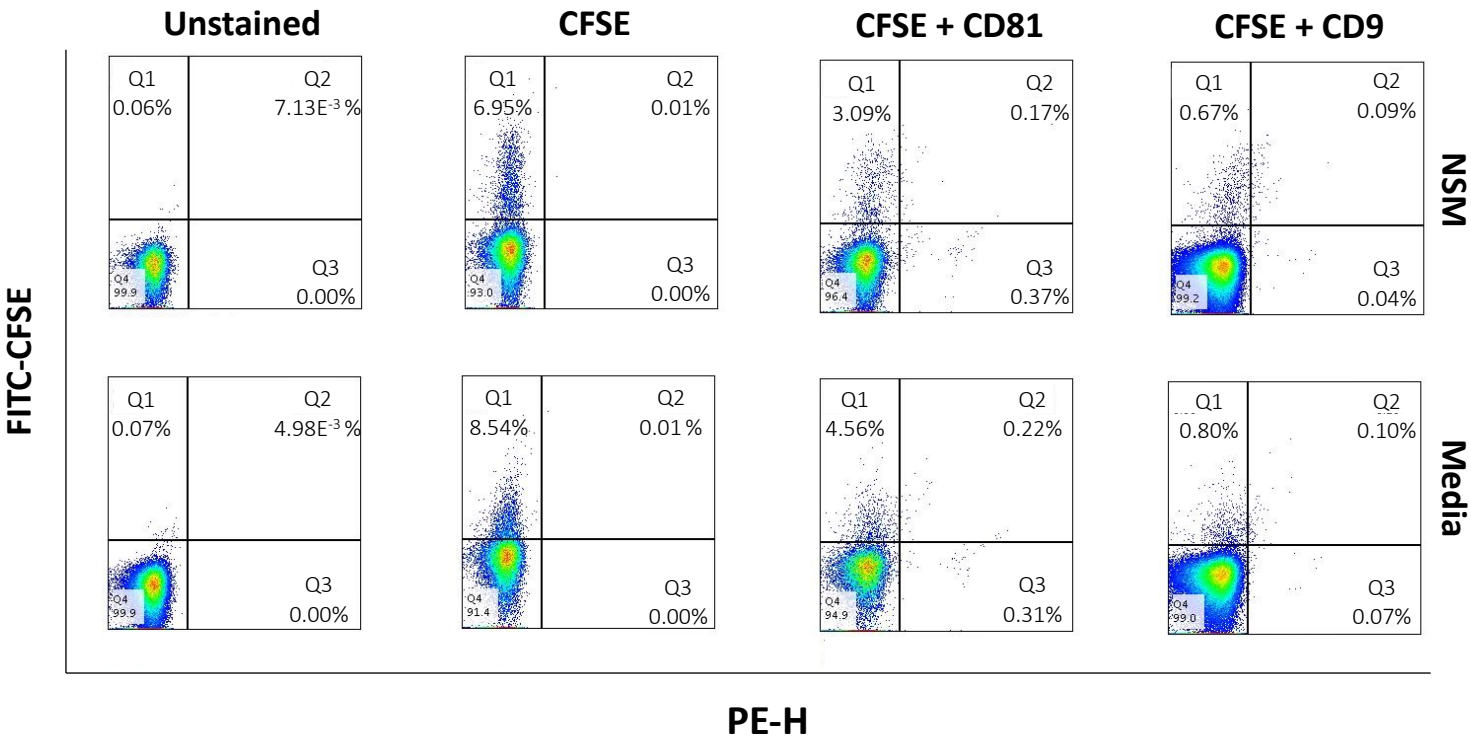

Figure 12. Naïve T-cell Supernatants at 0 hours of activation. *Treated and untreated culture media was applied to Naïve T-cell isolates and harvested immediately following its application to control for EV release resulting from the application of each suspension to the cells. NSM presents non-serum media (media lacking FBS) applied to T-cells. The top row consists of non-serum media applied to cells and immediately removed; while the bottom row consists of the same non-serum media supplemented with ultracentrifuged fetal bovine serum (FBS) media applied to cells and immediately removed. Across all stainings, it is apparent that some EVs are secreted just by the physical application of the media and that FBS associated EVs contribute to the population of secreted particles.*

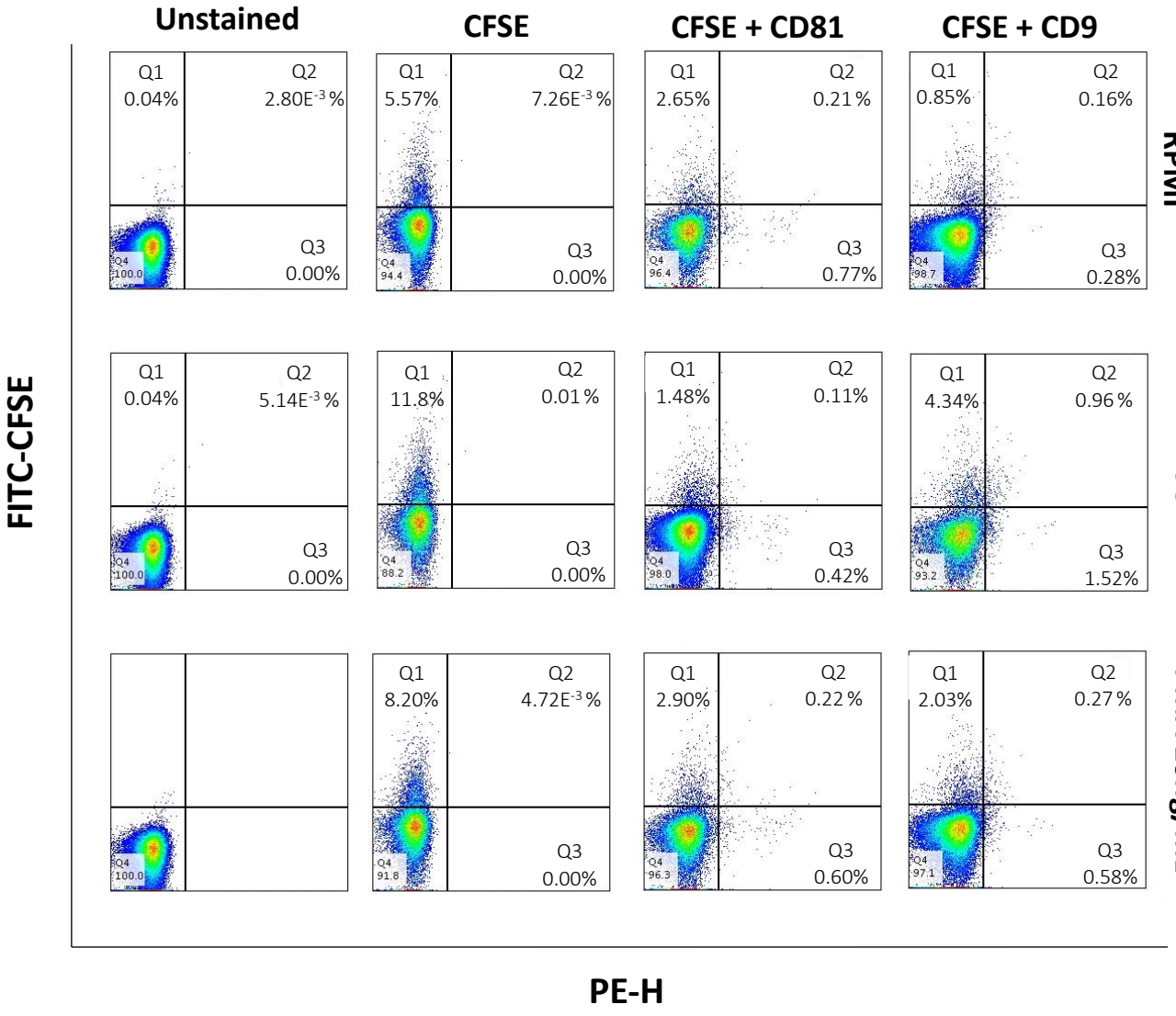

Figure 13. ***T-cell Supernatants 12-hours post activation.*** *Naïve T-cell treatments RPMI (Top), DMSO (Middle) and PMA 10ng/mL (Bottom) following 12 hours of incubation are arranged by row, while staining conditions are organized by column. The DMSO-treated cells report the highest percentage of CFSE-positive particles in column 2 (from the left). The RPMI untreated group had the highest percentage of CD81-positive particles in column 3. The DMSO treatment had the highest percentage of CD9 positive particles in column 4.*

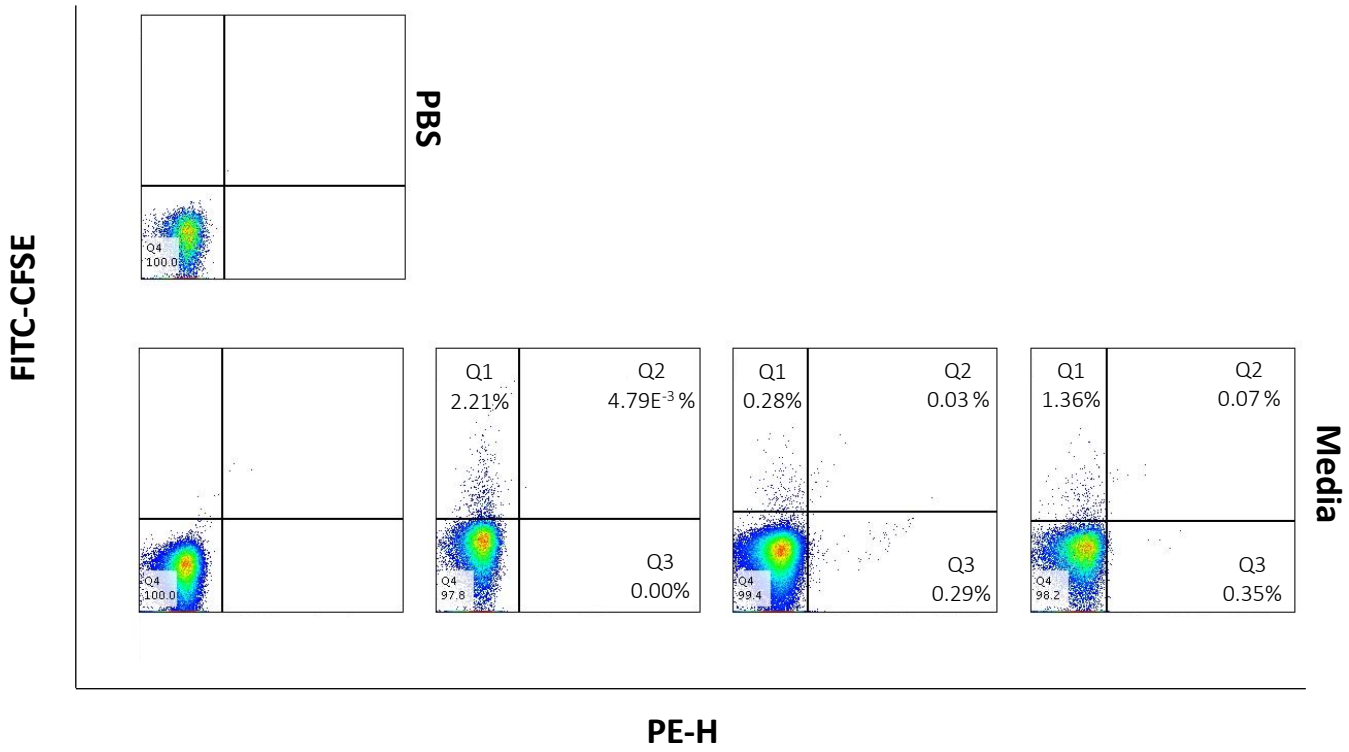

Figure 14. ***NFC Controls for 24-hour time point.*** *Staining controls for samples acquired at the 24-hour time point. A PBS control (Top Left) represents instrument background signal. Bottom row represents staining controls in media supplemented with ultracentrifuged FBS. Gating strategies follow the type of staining used for each treatment.*

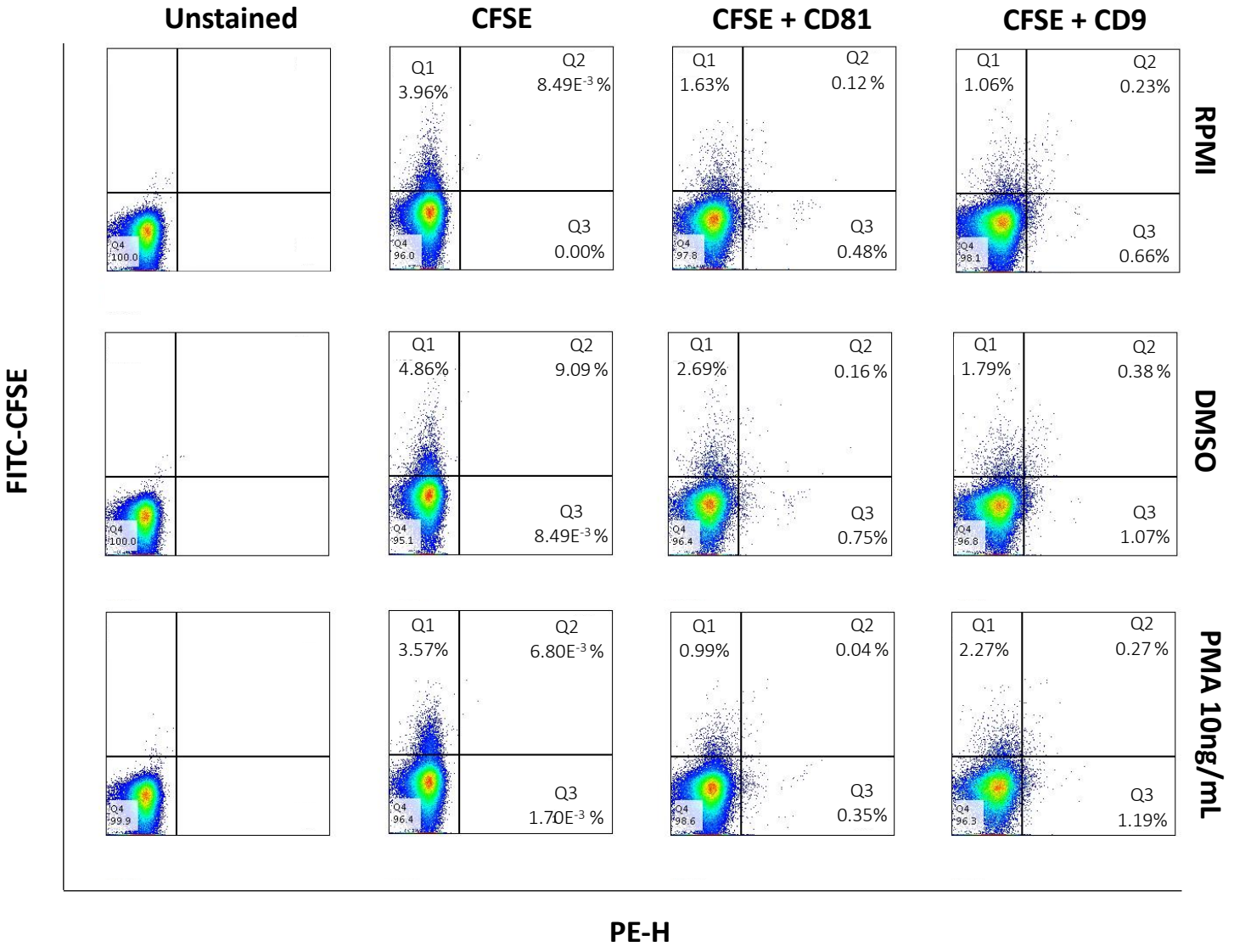

Figure 15. T-cell Supernatants 24 hours post activation. *Naïve T-cell treatments RPMI (Top), DMSO (Middle) and PMA 10ng/mL (Bottom) following 24 hours of incubation are arranged by row, while staining conditions are organized by column. The DMSO-treated cells report the highest percentages of CFSE-positive particles and CD81-positive particles in both columns 2 and 3 (from the left). In column 4, the PMA treated cells have a higher percentage of both CFSE-positive and CD9-positive particles.*

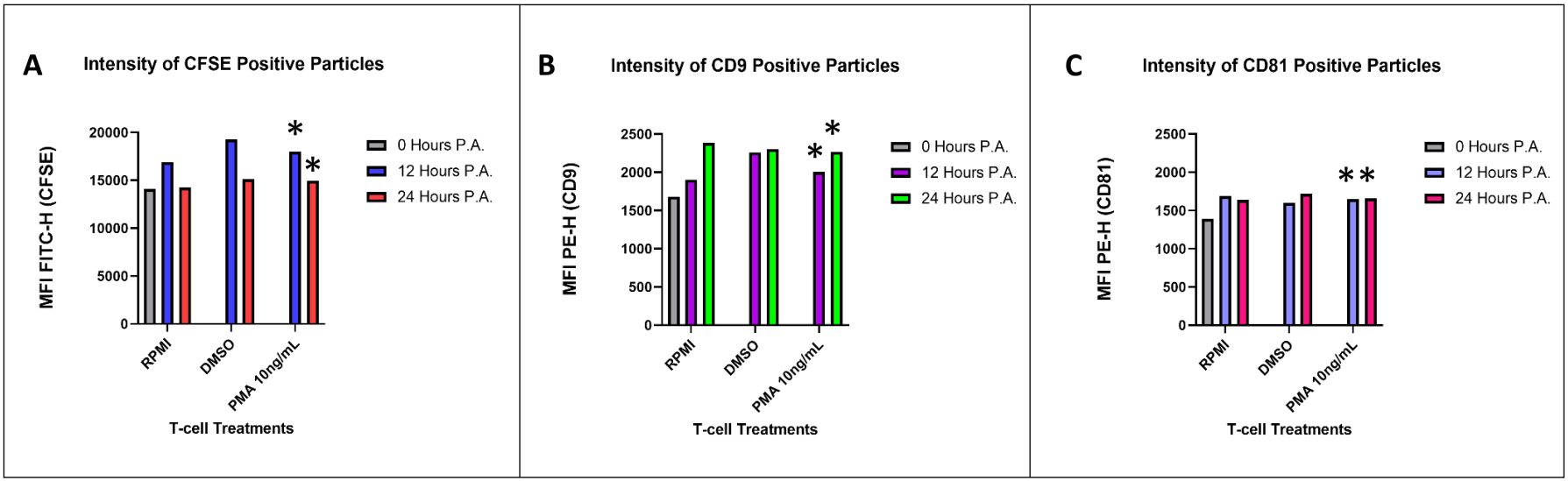

Figure 16. Analysis of Mean Fluorescent Intensities of Positively Labelled Secreted Particles at 0-, 12- and 24-Hour Time Points. *Particles secreted from treated T-cells were stained with CFSE and CD81 or CD9 fluorescent antibodies. The various T-cell treatments are listed on the x-axis. RPMI represents T-cells cultured in RPMI media containing "EV-depleted" FBS, DMSO represents T-cells treated in RPMI media containing "EV-depleted" FBS and a comparable concentration of DMSO to the PMA/I treated T-cells. Each treatment was assessed at the 12- and 24-hour time points post-activation (P.A.). Mean fluorescent intensity for the respective channel for each labelling method is listed on the y-axis. Positively labelled particles, as compared to controls, were gated on and the levels of fluorescent intensities assessed by FlowJo Software. One-way ANOVA analyses were performed for treatments pertaining to a given time point. Welsch's T-test was performed between the 12- and 24- hour PMA/I treatments, significance is denoted by an asterisk representing an obtained P value <0.0001. Experiment was not performed in replicate (n=1).* ***A)*** *One-way ANOVA analyses on CFSE-positive particles secreted within 12- and 24-hour time points were performed. Twelve-hour treatments mean fluorescent intensities in the FITC-H channel were found to be significant P <0.05 whereas 24-hour treatments were not found to be significantly different. The difference between mean fluorescent intensities between PMA/I treated T-cells at both time points by Welsch's T-test was found to be significant P< 0.0001.* ***B)*** *One-way ANOVA analyses on CD9-positive particles secreted within 12- and 24-hour time points were performed. Twelve-hour treatments mean fluorescent intensities in the PE-H channel were found to be significant P <0.05 whereas 24-hour treatments were not found to be significantly different. The difference between mean fluorescent intensities between PMA/I treated T-cells, at both time points, by Welsch's T-test was found to be significant P< 0.0001.* ***C)*** *One-way ANOVA analyses on CD81-positive particles secreted within 12- and 24-hour time points were performed. Treatments were not found to be significantly different. The difference between mean fluorescent intensities between PMA/I treated T-cells by Welsch's T-test, at both time points, was found to be significant P< 0.0001.*

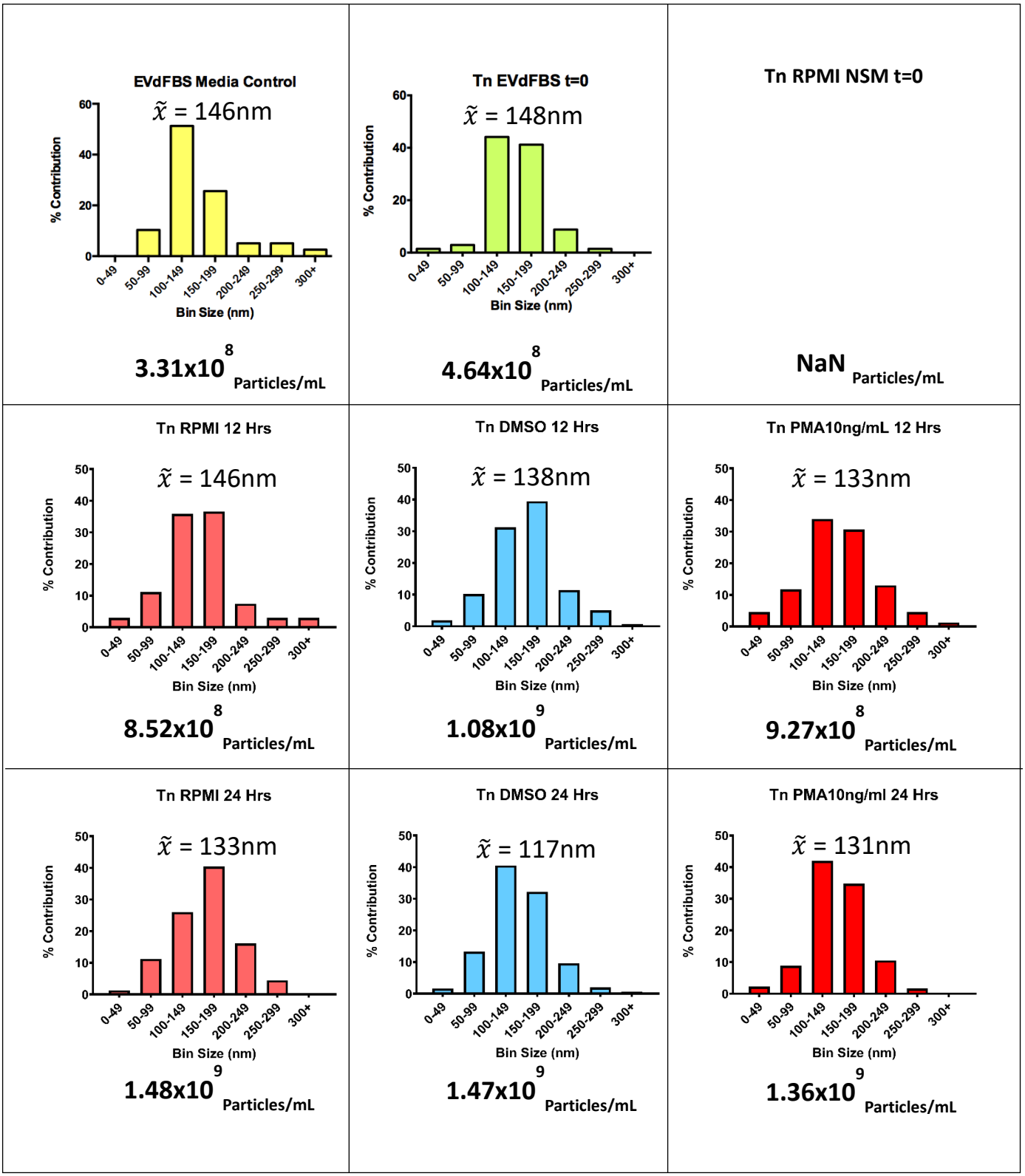

Figure 17. Nanoparticle Tracking Analysis of T-cell Supernatants at 0-, 12- and 24-hour time points. *Particle size distributions, median particle size and total particle concentration per treatment group where x-tilde represents the median particle size in a given sample and the particle count includes the dilution factor of the sample run on the instrument. Controls, treatment groups at the 12-hour time point and treatment groups at the 24-hour time point are arranged by row respectively. Supernatants harvested from Naïve T-cells are denoted with "Tn". In the 12-hour treatment, groups' median particle size appears to decrease with PMA treatment. While in the 24-hour treatment groups, median particle size appears to increase with treatment. Treatment groups in the bottom row, cultured for 24 hours, have larger concentrations of total particles than those of the 12-hour time point groups. Both PMA treatments were found to be statistically significant by Welsh's T-test (p<0.0001) compared to their respective time point, untreated RPMI and DMSO controls. Additionally, 24-Hr and 12Hr time point PMA treatments were found to be statistically significant by Welsh's T-test (p<0.0001). This experiment was not performed in replicate (n=1).*

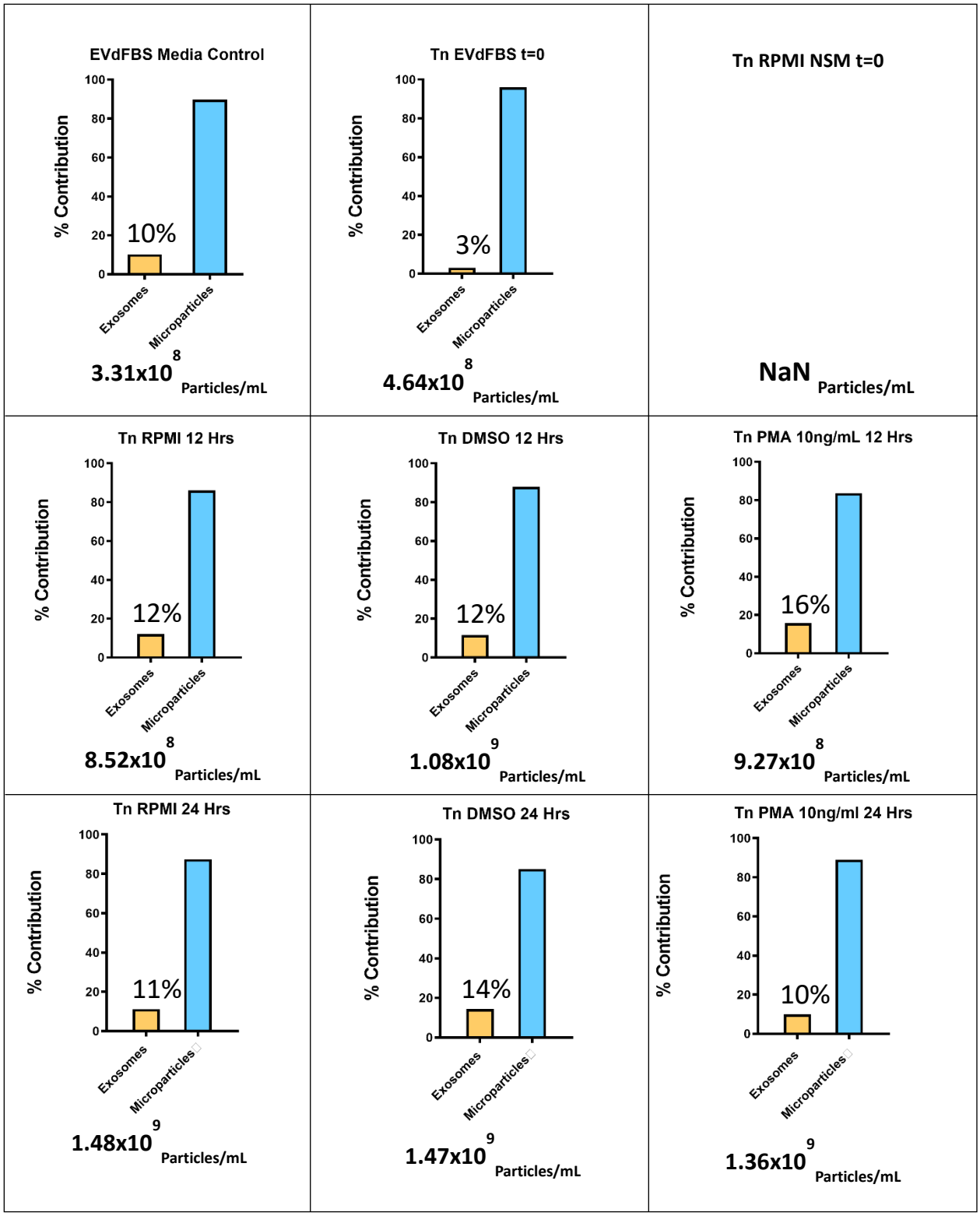

Figure 18. T-cell Supernatants from 0-, 12- and 24-hour time points Sorted by Particle Type by Size. *Treatment groups stored by biological particle size. Exosomes were defined by particles ranging from 40-100nm in size; while microparticles were defined as particles ranging from 100nm-1000nm. Controls, treatment groups at the 12-hour time point and treatment groups at the 24-hour time point are arranged by row, respectively. Supernatants harvested from Naïve T-cells are denoted with "Tn". In the 12-hour treatment groups, PMA treatment stimulated an increase in exosome-sized particles while, in the 24-hour treatment groups, the inverse was observed.*

Discussion

In this study, we sought to identify and quantify secreted particle populations from stimulated murine naïve $CD4^+$ T-cells. While further experiments are required to fully characterize EV secretions from T-cells under various stimulating conditions, many preliminary data presented here provide proof of concept with a strong likelihood of success. With this early work, the necessary conditions to optimally activate murine naïve $CD4^+$ T-cells with PMA was tested. While the concentration of PMA was determined, more experimentation is required to determine the optimal activation duration in order to achieve maximal particle output, minimize cell death, and minimize particle degradation before acquisitions. Additionally, NFC proved to be an effective tool in distinguishing between EV subsets. However, further optimization of acquisition parameters and fluorescent labelling are required.

The hypothesis of this study was that murine naïve $CD4^+$ T-cells would secrete specific EV patterns/profiles under immune stimulating conditions, and this was demonstrated by immune simulating PMA activations and quantification by NTA. Treatment of murine naïve $CD4^+$ T-cells with PMA almost always resulted in an increase in total particles and a negative shift in median particle size when compared to non-treated cells (Figures. 8, 9, 17 & 18). The exception was the PMA 10ng/mL group in Figure.10 which reported a higher median particle size than the non-treated cells. However, this observation is not found in Figure.16; thus, suggesting replicate experiments are needed to ascertain the nature of this result. While the observation that increasing internal Ca^{2+} stimulates exosome secretion pathways is not a new observation[162], the question remains why there is a selective negative shift in particle size that are released as opposed to a uniform increase in all particles released. This is likely due to the fact that exosome secretion pathway is a tightly controlled Ca^{2+}-dependent mechanism and increasing internal calcium levels is absolutely necessary in order to establish MVB fusion and exosome secretion, whereas microvesicle release is not as tightly regulated. The fact that there is a response in 100 – 149nm particle secretions to the calcium flux also adds to this point. In addition to negative shifts in particle size, increases in CD81+ and

CD9+ particles by NFC were also observed supporting the increase in exosomes secretion upon PMA/I stimulation (Figure. 13). These two tests were successful in identifying a trend that PMA/I stimulation leads to increases in total particle output and specific increases in exosome release on the basis of size and surface marker profiles.

The most significant limitation of these experiments is the statistical robustness of the analyses performed. For our experiments, the spleens from three separate female C57BL6/N mice were extracted and the isolated cells were pooled together and assessed once indicating an n of 1 (although 3 separate mice were used). It should be stated, however, that the nature of the project was exploratory as we sought to push the detection limits of NFC to see whether it would be possible to accurately discriminate particle subsets through surface antigen labelling. It is clear that the observable differences in surface antigen expression, following activation and in other experiments performed in our lab, were near or below the detection threshold of our flow cytometer. As such, the obtained results had very narrow dynamic range given their low abundance on the surface of our viral particles. An instrument with greater sensitivity, capable of detecting these minor changes in fluorescence while distinguishing background noise is therefore required for such small particle analyses to become mainstream.

While this work demonstrates a successful strategy, in order to correlate relevant stimuli with secreted particle populations, many considerations remain. Optimizations and further experimentation are needed to address these concerns and considerations. These experiments need to be repeated at least in triplicate to ensure the reliability of the observed “trends” and overcome the minor variabilities in secreted particles profiles, even though these results appear to follow previous observations[162]. Secondly, the amount of EVs being contributed from the culturing media need to be minimized. In some cases, media controls contributed roughly 30-35% of the total particles when comparing the media control to activated samples (Figures. 8 & 17). This is further demonstrated in the controls taken on the day of activation (t=0). In Figure. 16, the culturing medium containing EV depleted FBS

and immediately removed reported a total particle concentration of $4.64x10^8$ particles/mL while the RPMI non-serum media, placed on top of the cells and removed and diluted to the same factor, did not yield significant enough particle concentrations to be quantified by the ZetaView. This suggests that the FBS EV depletion protocol is not rigorous enough to eliminate a significant amount of contributing EVs. While ideally the culturing serum would not contribute to the total particles, this goal is unrealistic and other options should be considered. In the EV depletion of FBS, there is a reduction in total EV concentration. However, there is also a reduction in the beneficial proteins and growth factors needed to maintain cell viability. The use of EV depleted FBS will not favour healthy culturing conditions or cellular metabolic demands and will correlate to higher rates of cell death and increased particle release (microvesicles and apoptotic bodies). Instead, synthetic medias/serums should be considered and assessed for their impact on cell viability and levels of EV secretion as this will eliminate the possibility of contributing FBS-derived EVs, which overlap with secreted EVs of interest. Staining antibody concentration requires further optimization as populations of interest were not fully distinct or resolved. At the optimal antibody staining concentration, population subsets of interest would be fully separated (minimal overlap) from the background while not contributing significantly to the background or result in unspecific fluorescence.

With regards to activation length, more time points need to be observed to monitor particle secretions over time and observe cells and supernatants at peak activation and particle production. The length of activation and incubations requires optimization in order to observe the effect of activation on particle secretion in a timely manner and avoid EV degradation before acquisitions. There appears to be an “acceleration effect” in EV production by naïve CD4+ T-cells. Observed in Figure. 17, all treatments at the 24-hour time point appear to have very similar particle concentrations. Whereas, the 12-hour time point treatments demonstrate more disparity in the concentration of particles. When comparing treatment groups and analyzing secreted particle concentrations over time, for example the PMA 10ng/mL treated T-cells, by the 12-hour time point cells have produced $7.73x10^7$

particles/hour and by the 24-hour time point cells have produced $5.67x10^7$ particles/hour. Analyzing particle production in this fashion suggests that particle production is not a linear trend but more likely logarithmic where particle production drops off over time. This observation is easily explained by the principles of T-cell exhaustion in which cells lose their effector functions such as cytokine production and maintaining homeostasis, usually resulting in cell death. This also explains, in addition to the toxicity of PMA/I, why treated cells' produced particle concentrations are slightly lower compared to non-treated and control treatments as fewer viable cells means fewer secreted particles (Figures. 8 & 17)[163]. To truly be sure, cell cultures could be stained with known exhausted T-cell markers (CD43, CD69 and CD62L) and/or cytokine capture assays (IL-2, TNFα) and run by flow cytometry to assess the proportion of live/dead, activated/non-activated and exhausted T-cells post activation. Additional time points around the 12-hour time point need to be assessed for peak particle production.

While this work demonstrates some preliminary steps in identifying patterns in particle secretions from immune cells, further work is necessary to characterize the heterogeneity of the secreted particle populations under immunologically relevant conditions. Endogenous retrovirus presence in activated and control supernatants needs to be addressed and assessed using the same quantification techniques. As demonstrated by Kwon *et al*. 2011 stimulating primary lymphoid cells (T- and B-cells) using lipopolysaccharide lead to increased secretion of Moloney murine leukemia ERVs[164]. As such, these particle subsets need to be quantified effectively in conjunction with EVs as they contribute to the total particles secreted by murine naïve CD4+ T-cells. Typically, murine viruses (including ERVs) can be seen by side scatter by NFC/flow virometry as previously demonstrated by our lab and in unpublished results. Unfortunately, results shown here do not effectively demonstrate ERVs by side scatter. This may be a result of the 1:100 dilution used to run samples by NFC as this would make discrimination of the discrete population perhaps too dilute, to overcome the typical background signals observed by side scatter. As these are uninfected samples, what should be expected is a dense homogenous population located within the background noise in non-CFSE stained

control samples which would resemble the scatter profile of an infected sample; however, this population would have to be of endogenous origin and likely to be ERVs. One potential solution would be to increase the concentration used during acquisitions. However, this does not play to the strengths of NFC as some disadvantages of NFC are coincidental events during acquisitions (two or more particles travelling past the point of measurement at a given time) and the limits of detection with regards to the size of particles[18]. With this in mind, increasing the concentration of particles for acquisition will lead to increased coincidental events, increased background signals and therefore skew results which would underestimate the true result and make distinguishing distinct populations (EVs from VLPs, ERVs and background signals) very difficult. If methods existed to label the gag protein of the capsid internally, ERV populations could be further discriminated from background signals. This would be an exceptionally invaluable technique to characterize ERV populations and test and separate exogenous MLV infection, from ERVs, in future immunological assays in conjunction with additional testing methods.

An additional level/dimension of ERV secretion, which can be explored and requires consideration, is the type of murine model used. For the purposes of the experiments detailed here, female C57BL6 mice were acquired from Charles River Laboratories formally denoted as C57BL6/N. Future experiments, in addition to including replicate experiments, should include male along side female C57BL6/N mice to enable comparisons to be made and avoid sex-based bias[165]. Recent studies revealed that non-ecotropic ERVs were not repressed in C57BL6/N strains resulting in increased expression of ERVs and ERV-related products compared to Jackson Laboratory mouse strain C57BL6/J[166]. This finding suggests special consideration is necessary in the selection of murine models for ERV-related research. This is an important point of interest for further investigation to determine ERV secretion profiles under stimulatory conditions in both strains, used as a reduced ERV control in the case of C57BL6/J and ascertain the validity of the C57BL6/N and /J strains in ERV experiments and research.

Following optimization of culturing conditions, activation conditions and staining and acquisition techniques, the next steps for this project are to explore other immunologically relevant stimuli, assess and correlate secreted particle profiles with specific T-helper cell subset responses (Th1, Th2 and Th17), and identifying the surface markers presented by EVs and ERVs through staining assays. Uncovering and relating specific secreted particle profiles to specifically stimulated immune pathways such as JAK-STAT and NFκB pathways is at the core of this project. This work would help clarify the roles immune stimulation plays on EV secretion, the additional roles EVs play in immunologically relevant microenvironments, and serve as a reference when using EVs as a swift clinical diagnostic tool or biomarker of disease.

Conclusion

Herein, we demonstrated early steps into the analysis of discrete particle populations secreted by murine immune cells. Nanoscale Flow Cytometry and Nanoparticle Tracking Analysis are both incredibly useful tools which enable studies of the heterogenous microscopic particles secreted under various stimulatory conditions to be assessed. Using both NFC and NTA to analyze particles secreted by murine naïve $CD4^+$ T-cells, some preliminary trends were observed. We showed that mimicking a naïve T-cell activation using PMA and Ionomycin upregulated the total number of particles secreted and specifically favoured the secretion of smaller particles carrying known exosome biomarkers. This means perhaps the exosome pathway is being specifically upregulated. This project outlines a workflow which can be followed to assess other types of stimulatory conditions which represent important immune responses to begin profiling secretion patterns and potentially creating a library of known particle profiles. Documenting and categorizing known secretion profiles from different cell types and stimulants would be extremely invaluable in the potential development of novel screening, diagnostic and targeted therapies. The likelihood of the project's success is exciting. However, there are

some challenges to be overcome to fully address all the secreted particle subsets. Specifically, discriminating ERVs from other particles like VLPs and EVs and invading viruses from relevant assays is currently not available using current staining and acquisition techniques by NFC. While this work demonstrates many preliminary steps and results, there is still much work required to fully achieve the initial scope defined in this project. The potential implications of this work would unlock and reveal crucial information into EV behaviour, physiology, immune responses, and the development of novel diagnostic tools. This knowledge would help in developing strategies to understand the roles EVs play in pathology which, in turn, would enable cancers, infections, and autoimmune disorders to be better understood and rapidly identified.

References

1. Robbins, P. D. & Morelli, A. E. Regulation of immune responses by extracellular vesicles. *Nature Reviews Immunology* (2014) doi:10.1038/nri3622.

2. Paolicelli, R. C., Bergamini, G. & Rajendran, L. Cell-to-cell Communication by Extracellular Vesicles: Focus on Microglia. *Neuroscience* **405**, 148–157 (2019).

3. Cesselli, D. *et al.* Extracellular vesicles: How drug and pathology interfere with their biogenesis and function. *Frontiers in Physiology* (2018) doi:10.3389/fphys.2018.01394.

4. Wurdinger, T. *et al.* Extracellular Vesicles and Their Convergence with Viral Pathways. *Advances in Virology* (2012) doi:10.1155/2012/767694.

5. Nolte-'t Hoen, E., Cremer, T., Gallo, R. C. & Margolis, L. B. Extracellular vesicles and viruses: Are they close relatives? *Proc. Natl. Acad. Sci. U. S. A.* **113**, 9155–9161 (2016).

6. Jena, B. P. Secretion machinery at the cell plasma membrane. *Curr. Opin. Struct. Biol.* **17**, 437–443 (2007).

7. Cohen, F. S. How Viruses Invade Cells. *Biophys. J.* **110**, 1028–1032 (2016).

8. Ståhl, A.-L., Johansson, K., Mossberg, M., Kahn, R. & Karpman, D. Exosomes and microvesicles in normal physiology, pathophysiology, and renal diseases. *Pediatr. Nephrol.* **34**, 11–30 (2019).

9. Ryan, F. P. Human endogenous retroviruses in health and disease: a symbiotic perspective. *J. R. Soc. Med.* **97**, 560–565 (2004).

10. Grandi, N. & Tramontano, E. HERV envelope proteins: Physiological role and pathogenic potential in cancer and autoimmunity. *Frontiers in Microbiology* (2018) doi:10.3389/fmicb.2018.00462.

11. Fauquet, C. M. TAXONOMY, CLASSIFICATION AND NOMENCLATURE OF VIRUSES. *Encycl. Virol.* 1730–1756 (1999) doi:10.1006/rwvi.1999.0277.

12. McFadden, G., Mohamed, M. R., Rahman, M. M. & Bartee, E. Cytokine determinants of viral tropism. *Nat. Rev. Immunol.* **9**, 645–655 (2009).

13. Traylen, C. M. *et al.* Virus reactivation: a panoramic view in human infections. *Future Virol.* **6**, 451–463 (2011).

14. Speck, S. H. & Ganem, D. Viral latency and its regulation: lessons from the gamma-herpesviruses. *Cell Host Microbe* **8**, 100–115 (2010).

15. Gill, S., Catchpole, R. & Forterre, P. Extracellular membrane vesicles in the three domains of life and beyond. *FEMS Microbiol. Rev.* (2019)

doi:10.1093/femsre/fuy042.

16. Willms, E., Cabañas, C., Mäger, I., Wood, M. J. A. & Vader, P. Extracellular Vesicle Heterogeneity: Subpopulations, Isolation Techniques, and Diverse Functions in Cancer Progression . *Frontiers in Immunology* vol. 9 738 (2018).

17. Margolis, L. & Sadovsky, Y. The biology of extracellular vesicles: The known unknowns. *PLOS Biol.* **17**, e3000363 (2019).

18. Chiang, C. & Chen, C. Toward characterizing extracellular vesicles at a single-particle level. *J. Biomed. Sci.* **26**, 9 (2019).

19. Koniusz, S. *et al.* Extracellular Vesicles in Physiology, Pathology, and Therapy of the Immune and Central Nervous System, with Focus on Extracellular Vesicles Derived from Mesenchymal Stem Cells as Therapeutic Tools . *Frontiers in Cellular Neuroscience* vol. 10 109 (2016).

20. Lesbats, P., Engelman, A. N. & Cherepanov, P. Retroviral DNA Integration. *Chemical Reviews* (2016) doi:10.1021/acs.chemrev.6b00125.

21. Battistini, A. & Sgarbanti, M. HIV-1 latency: an update of molecular mechanisms and therapeutic strategies. *Viruses* **6**, 1715–1758 (2014).

22. Tang, V. A., Renner, T. M., Fritzsche, A. K., Burger, D. & Langlois, M.-A. Single-Particle Discrimination of Retroviruses from Extracellular Vesicles by Nanoscale Flow Cytometry. *Sci. Rep.* **7**, 17769 (2017).

23. Coffin, J. M., Hughes, S. & Varmus, H. E. *Retroviruses*. (New York: Cold Spring Harbor Laboratory Press, 1997).

24. Poletti, V. & Mavilio, F. Interactions between Retroviruses and the Host Cell Genome. *Mol. Ther. Methods Clin. Dev.* **8**, 31–41 (2017).

25. Nisole, S. & Saïb, A. Early steps of retrovirus replicative cycle. *Retrovirology* (2004) doi:10.1186/1742-4690-1-9.

26. Overbaugh, J., Miller, A. D. & Eiden, M. V. Receptors and entry cofactors for retroviruses include single and multiple transmembrane-spanning proteins as well as newly described glycophosphatidylinositol-anchored and secreted proteins. *Microbiol. Mol. Biol. Rev.* **65**, 371–389 (2001).

27. Wilen, C. B., Tilton, J. C. & Doms, R. W. HIV: cell binding and entry. *Cold Spring Harb. Perspect. Med.* **2**, a006866 (2012).

28. Kubo, Y., Hayashi, H., Matsuyama, T., Sato, H. & Yamamoto, N. Retrovirus entry by endocytosis and cathepsin proteases. *Advances in Virology* (2012) doi:10.1155/2012/640894.

29. Hughes, S. H. Reverse Transcription of Retroviruses and LTR Retrotransposons. *Microbiol. Spectr.* **3**, MDNA3-2014 (2015).

30. Iordanskiy, S. & Bukrinsky, M. Reverse transcription complex: the key player

of the early phase of HIV replication. *Future Virol.* **2**, 49–64 (2007).

31. Matreyek, K. A. & Engelman, A. Viral and cellular requirements for the nuclear entry of retroviral preintegration nucleoprotein complexes. *Viruses* **5**, 2483–2511 (2013).

32. Miklík, D., Šenigl, F. & Hejnar, J. Proviruses with Long-Term Stable Expression Accumulate in Transcriptionally Active Chromatin Close to the Gene Regulatory Elements: Comparison of ASLV-, HIV- and MLV-Derived Vectors. *Viruses* **10**, 116 (2018).

33. Siliciano, R. F. & Greene, W. C. HIV latency. *Cold Spring Harb. Perspect. Med.* **1**, a007096–a007096 (2011).

34. Uren, A. G., Kool, J., Berns, A. & van Lohuizen, M. Retroviral insertional mutagenesis: past, present and future. *Oncogene* **24**, 7656–7672 (2005).

35. Grandi, N. & Tramontano, E. Human Endogenous Retroviruses Are Ancient Acquired Elements Still Shaping Innate Immune Responses . *Frontiers in Immunology* vol. 9 2039 (2018).

36. Basyuk, E. *et al.* Retroviral genomic RNAs are transported to the plasma membrane by endosomal vesicles. *Dev. Cell* (2003) doi:10.1016/S1534-5807(03)00188-6.

37. Moore, M. D. & Hu, W. S. HIV-1 RNA dimerization: It takes two to tango. *AIDS Rev.* **11**, 91–102 (2009).

38. Berlioz, C. & Darlix, J. L. An internal ribosomal entry mechanism promotes translation of murine leukemia virus gag polyprotein precursors. *J. Virol.* **69**, 2214–2222 (1995).

39. Yilmaz, A., Bolinger, C. & Boris-Lawrie, K. Retrovirus translation initiation: Issues and hypotheses derived from study of HIV-1. *Curr. HIV Res.* **4**, 131–139 (2006).

40. Olson, E. D. & Musier-Forsyth, K. Retroviral Gag protein-RNA interactions: Implications for specific genomic RNA packaging and virion assembly. *Semin. Cell Dev. Biol.* **86**, 129–139 (2019).

41. Cochrane, A. W., McNally, M. T. & Mouland, A. J. The retrovirus RNA trafficking granule: from birth to maturity. *Retrovirology* **3**, 18 (2006).

42. Murakami, T. Retroviral env glycoprotein trafficking and incorporation into virions. *Mol. Biol. Int.* **2012**, 682850 (2012).

43. Pincetic, A. & Leis, J. The Mechanism of Budding of Retroviruses From Cell Membranes. *Adv. Virol.* **2009**, 6239691–6239699 (2009).

44. Thali, M. The roles of tetraspanins in HIV-1 replication. *Curr. Top. Microbiol. Immunol.* **339**, 85–102 (2009).

45. Mattei, S., Schur, F. K. M. & Briggs, J. A. G. Retrovirus maturation—an

extraordinary structural transformation. *Curr. Opin. Virol.* **18**, 27–35 (2016).

46. Doitsh, G. & Greene, W. C. Dissecting How CD4 T Cells Are Lost During HIV Infection. *Cell Host Microbe* **19**, 280–291 (2016).

47. Halo, J. V *et al.* Origin and recent expansion of an endogenous gammaretroviral lineage in domestic and wild canids. *Retrovirology* **16**, 6 (2019).

48. Lescot, M. *et al.* Reverse transcriptase genes are highly abundant and transcriptionally active in marine plankton assemblages. *ISME J.* **10**, 1134–1146 (2016).

49. Gifford, R. J. *et al.* Nomenclature for endogenous retrovirus (ERV) loci. *Retrovirology* **15**, 59 (2018).

50. Tokuyama, M. *et al.* ERVmap analysis reveals genome-wide transcription of human endogenous retroviruses. *Proc. Natl. Acad. Sci.* **115**, 12565 LP – 12572 (2018).

51. Nelson, P. N. *et al.* Demystified. Human endogenous retroviruses. *Mol. Pathol.* **56**, 11–18 (2003).

52. Nishant, K. T., Singh, N. D. & Alani, E. Genomic mutation rates: what high-throughput methods can tell us. *Bioessays* **31**, 912–920 (2009).

53. Meyer, T. J., Rosenkrantz, J. L., Carbone, L. & Chavez, S. L. Endogenous Retroviruses: With Us and against Us. *Front. Chem.* **5**, 23 (2017).

54. Stocking, C. & Kozak, C. A. Endogenous retroviruses: Murine endogenous retroviruses. *Cellular and Molecular Life Sciences* (2008) doi:10.1007/s00018-008-8497-0.

55. Hsu, K. *et al.* Inherently variable responses to glucocorticoid stress among endogenous retroviruses isolated from 23 mouse strains. *Biochim. Biophys. Acta - Mol. Basis Dis.* (2017) doi:10.1016/j.bbadis.2016.10.026.

56. Elbarbary, R. A., Lucas, B. A. & Maquat, L. E. Retrotransposons as regulators of gene expression. *Science* **351**, aac7247–aac7247 (2016).

57. Dodonova, S. O., Prinz, S., Bilanchone, V., Sandmeyer, S. & Briggs, J. A. G. Structure of the Ty3/Gypsy retrotransposon capsid and the evolution of retroviruses. *Proc. Natl. Acad. Sci.* **116**, 10048 LP – 10057 (2019).

58. Stoye, J. P. Endogenous retroviruses: Still active after all these years? *Curr. Biol.* **11**, R914–R916 (2001).

59. Kozak, C. A. Origins of the endogenous and infectious laboratory mouse gammaretroviruses. *Viruses* (2015) doi:10.3390/v7010001.

60. Bamunusinghe, D. *et al.* Sequence Diversity, Intersubgroup Relationships, and Origins of the Mouse Leukemia Gammaretroviruses of Laboratory and Wild Mice. *J. Virol.* **90**, 4186 LP – 4198 (2016).

61. Bamunusinghe, D., Liu, Q., Lu, X., Oler, A. & Kozak, C. A. Endogenous Gammaretrovirus Acquisition in Mus musculus Subspecies Carrying Functional Variants of the XPR1 Virus Receptor. *J. Virol.* **87**, 9845 LP – 9855 (2013).

62. Farrell, K. B. & Eiden, M. V. Dissection of gammaretroviral receptor function by using type III phosphate transporters as models. *J. Virol.* **79**, 9332–9336 (2005).

63. Boi, S. *et al.* Endogenous retroviruses mobilized during friend murine leukemia virus infection. *Virology* (2016) doi:10.1016/j.virol.2016.07.009.

64. Greenberger, J. S., Phillips, S. M., Stephenson, J. R. & Aaronson, S. A. Induction of Mouse Type-C RNA Virus by Lipopolysaccharide. *J. Immunol.* **115**, 317 LP – 320 (1975).

65. Gonzalez-Hernandez, M. J. *et al.* Expression of Human Endogenous Retrovirus Type K (HML-2) Is Activated by the Tat Protein of HIV-1. *J. Virol.* **86**, 7790 LP – 7805 (2012).

66. Toufaily, C., Landry, S., Leib-Mosch, C., Rassart, E. & Barbeau, B. Activation of LTRs from different human endogenous retrovirus (HERV) families by the HTLV-1 tax protein and T-cell activators. *Viruses* (2011) doi:10.3390/v3112146.

67. Contreras-Galindo, R. *et al.* Human Endogenous Retrovirus Type K (HERV-K) Particles Package and Transmit HERV-K–Related Sequences. *J. Virol.* (2015) doi:10.1128/jvi.00544-15.

68. Johanning, G. L. *et al.* Expression of human endogenous retrovirus-K is strongly associated with the basal-like breast cancer phenotype. *Sci. Rep.* (2017) doi:10.1038/srep41960.

69. Doyle, L. M. & Wang, M. Z. Overview of Extracellular Vesicles, Their Origin, Composition, Purpose, and Methods for Exosome Isolation and Analysis. *Cells* **8**, 727 (2019).

70. Tang, T.-T., Lv, L.-L., Lan, H.-Y. & Liu, B.-C. Extracellular Vesicles: Opportunities and Challenges for the Treatment of Renal Diseases. *Front. Physiol.* **10**, 226 (2019).

71. Xu, X., Lai, Y. & Hua, Z. C. Apoptosis and apoptotic body: Disease message and therapeutic target potentials. *Bioscience Reports* (2019) doi:10.1042/BSR20180992.

72. Jiang, L. *et al.* Determining the contents and cell origins of apoptotic bodies by flow cytometry. *Sci. Rep.* (2017) doi:10.1038/s41598-017-14305-z.

73. Elmore, S. Apoptosis: a review of programmed cell death. *Toxicol. Pathol.* **35**, 495–516 (2007).

74. Zhang, N. & Bevan, M. J. CD8(+) T cells: foot soldiers of the immune system. *Immunity* **35**, 161–168 (2011).

75. Takeuchi, A. & Saito, T. CD4 CTL, a Cytotoxic Subset of CD4(+) T Cells, Their Differentiation and Function. *Front. Immunol.* **8**, 194 (2017).

76. Boivin, W. A., Cooper, D. M., Hiebert, P. R. & Granville, D. J. Intracellular versus extracellular granzyme B in immunity and disease: challenging the dogma. *Lab. Investig.* **89**, 1195–1220 (2009).

77. Vivier, E., Tomasello, E., Baratin, M., Walzer, T. & Ugolini, S. Functions of natural killer cells. *Nat. Immunol.* **9**, 503–510 (2008).

78. Battistelli, M. & Falcieri, E. Apoptotic Bodies: Particular Extracellular Vesicles Involved in Intercellular Communication. *Biology (Basel).* **9**, 21 (2020).

79. van Genderen, H. O., Kenis, H., Hofstra, L., Narula, J. & Reutelingsperger, C. P. M. Extracellular annexin A5: Functions of phosphatidylserine-binding and two-dimensional crystallization. *Biochimica et Biophysica Acta - Molecular Cell Research* (2008) doi:10.1016/j.bbamcr.2008.01.030.

80. Gerke, V. & Moss, S. E. Annexins: From Structure to Function. *Physiol. Rev.* **82**, 331–371 (2002).

81. Logue, S. E., Elgendy, M. & Martin, S. J. Expression, purification and use of recombinant annexin V for the detection of apoptotic cells. *Nat. Protoc.* **4**, 1383–1395 (2009).

82. Muralidharan-Chari, V., Clancy, J. W., Sedgwick, A. & D'Souza-Schorey, C. Microvesicles: mediators of extracellular communication during cancer progression. *J. Cell Sci.* **123**, 1603 LP – 1611 (2010).

83. Chen, Y., Li, G. & Liu, M.-L. Microvesicles as Emerging Biomarkers and Therapeutic Targets in Cardiometabolic Diseases. *Genomics. Proteomics Bioinformatics* **16**, 50–62 (2018).

84. Kreger, B. T., Dougherty, A. L., Greene, K. S., Cerione, R. A. & Antonyak, M. A. Microvesicle Cargo and Function Changes upon Induction of Cellular Transformation. *J. Biol. Chem.* **291**, 19774–19785 (2016).

85. Camussi, G., Deregibus, M. C., Bruno, S., Cantaluppi, V. & Biancone, L. Exosomes/microvesicles as a mechanism of cell-to-cell communication. *Kidney Int.* **78**, 838–848 (2010).

86. Colombo, M., Raposo, G. & Théry, C. Biogenesis, Secretion, and Intercellular Interactions of Exosomes and Other Extracellular Vesicles. *Annu. Rev. Cell Dev. Biol.* **30**, 255–289 (2014).

87. Huotari, J. & Helenius, A. Endosome maturation. *EMBO Journal* (2011) doi:10.1038/emboj.2011.286.

88. Hessvik, N. P. & Llorente, A. Current knowledge on exosome biogenesis and

release. *Cell. Mol. Life Sci.* **75**, 193–208 (2018).

89. Nabi, I. R. & Le, P. U. Caveolae/raft-dependent endocytosis. *J. Cell Biol.* **161**, 673–677 (2003).

90. Schmidt, O. & Teis, D. The ESCRT machinery. *Curr. Biol.* **22**, R116–R120 (2012).

91. Henne, W. M., Stenmark, H. & Emr, S. D. Molecular mechanisms of the membrane sculpting ESCRT pathway. *Cold Spring Harb. Perspect. Biol.* **5**, a016766 (2013).

92. Hu, Y. B., Dammer, E. B., Ren, R. J. & Wang, G. The endosomal-lysosomal system: From acidification and cargo sorting to neurodegeneration. *Translational Neurodegeneration* (2015) doi:10.1186/s40035-015-0041-1.

93. Wandinger-Ness, A. & Zerial, M. Rab proteins and the compartmentalization of the endosomal system. *Cold Spring Harb. Perspect. Biol.* **6**, a022616–a022616 (2014).

94. Lodish, H. *et al. Molecular Cell Biology, 4th edition*. (2000).

95. Schwartz, S. L., Cao, C., Pylypenko, O., Rak, A. & Wandinger-Ness, A. Rab GTPases at a glance. *J. Cell Sci.* **120**, 3905 LP – 3910 (2007).

96. Pylypenko, O., Hammich, H., Yu, I.-M. & Houdusse, A. Rab GTPases and their interacting protein partners: Structural insights into Rab functional diversity. *Small GTPases* **9**, 22–48 (2018).

97. Hutagalung, A. H. & Novick, P. J. Role of Rab GTPases in membrane traffic and cell physiology. *Physiol. Rev.* **91**, 119–149 (2011).

98. Han, J., Pluhackova, K. & Böckmann, R. A. The Multifaceted Role of SNARE Proteins in Membrane Fusion . *Frontiers in Physiology* vol. 8 5 (2017).

99. Catalano, M. & O'Driscoll, L. Inhibiting extracellular vesicles formation and release: a review of EV inhibitors. *J. Extracell. vesicles* **9**, 1703244 (2019).

100. van der Vlist, E. J. *et al.* CD4(+) T cell activation promotes the differential release of distinct populations of nanosized vesicles. *J. Extracell. vesicles* **1**, 10.3402/jev.v1i0.18364 (2012).

101. Villarroya-Beltri, C. *et al.* ISGylation controls exosome secretion by promoting lysosomal degradation of MVB proteins. *Nat. Commun.* **7**, 13588 (2016).

102. Villarroya-Beltri, C., Guerra, S. & Sánchez-Madrid, F. ISGylation – a key to lock the cell gates for preventing the spread of threats. *J. Cell Sci.* **130**, 2961 LP – 2969 (2017).

103. Chalmin, F. *et al.* Membrane-associated Hsp72 from tumor-derived exosomes mediates STAT3-dependent immunosuppressive function of mouse and human myeloid-derived suppressor cells. *J. Clin. Invest.* **120**, 457–471 (2010).

104. Horibe, S., Tanahashi, T., Kawauchi, S., Murakami, Y. & Rikitake, Y. Mechanism of recipient cell-dependent differences in exosome uptake. *BMC Cancer* **18**, 47 (2018).

105. Lane, R. E., Korbie, D., Hill, M. M. & Trau, M. Extracellular vesicles as circulating cancer biomarkers: opportunities and challenges. *Clin. Transl. Med.* **7**, 14 (2018).

106. Dickhout, A. & Koenen, R. R. Extracellular Vesicles as Biomarkers in Cardiovascular Disease; Chances and Risks . *Frontiers in Cardiovascular Medicine* vol. 5 113 (2018).

107. Luan, X. *et al.* Engineering exosomes as refined biological nanoplatforms for drug delivery. *Acta Pharmacol. Sin.* **38**, 754–763 (2017).

108. Akuma, P., Okagu, O. D. & Udenigwe, C. C. Naturally Occurring Exosome Vesicles as Potential Delivery Vehicle for Bioactive Compounds . *Frontiers in Sustainable Food Systems* vol. 3 23 (2019).

109. Mulcahy, L. A., Pink, R. C. & Carter, D. R. F. Routes and mechanisms of extracellular vesicle uptake. *J. Extracell. vesicles* **3**, 10.3402/jev.v3.24641 (2014).

110. Maas, S. L. N., Breakefield, X. O. & Weaver, A. M. Extracellular Vesicles: Unique Intercellular Delivery Vehicles. *Trends Cell Biol.* **27**, 172–188 (2017).

111. Raposo, G. & Stoorvogel, W. Extracellular vesicles: exosomes, microvesicles, and friends. *J. Cell Biol.* **200**, 373–383 (2013).

112. Cibrián, D. & Sánchez-Madrid, F. CD69: from activation marker to metabolic gatekeeper. *Eur. J. Immunol.* **47**, 946–953 (2017).

113. Yáñez-Mó, M. *et al.* Biological properties of extracellular vesicles and their physiological functions. *J. Extracell. vesicles* **4**, 27066 (2015).

114. Rybak, K. & Robatzek, S. Functions of Extracellular Vesicles in Immunity and Virulence. *Plant Physiol.* **179**, 1236–1247 (2019).

115. O'Brien, K., Breyne, K., Ughetto, S., Laurent, L. C. & Breakefield, X. O. RNA delivery by extracellular vesicles in mammalian cells and its applications. *Nat. Rev. Mol. Cell Biol.* **21**, 585–606 (2020).

116. Barnes, B. J. & Somerville, C. C. Modulating Cytokine Production via Select Packaging and Secretion From Extracellular Vesicles. *Front. Immunol.* **11**, 1040 (2020).

117. Seif, F. *et al.* The role of JAK-STAT signaling pathway and its regulators in the fate of T helper cells. *Cell Commun. Signal.* **15**, 23 (2017).

118. Liu, T., Zhang, L., Joo, D. & Sun, S.-C. NF-κB signaling in inflammation. *Signal Transduct. Target. Ther.* **2**, 17023 (2017).

119. O'Brien, J., Hayder, H., Zayed, Y. & Peng, C. Overview of MicroRNA

Biogenesis, Mechanisms of Actions, and Circulation . *Frontiers in Endocrinology* vol. 9 402 (2018).

120. Urbanelli, L. *et al.* The Role of Extracellular Vesicles in Viral Infection and Transmission. *Vaccines* **7**, 102 (2019).

121. Votteler, J. & Sundquist, W. I. Virus budding and the ESCRT pathway. *Cell Host Microbe* **14**, 232–241 (2013).

122. Grgacic, E. V. L. & Anderson, D. A. Virus-like particles: passport to immune recognition. *Methods* **40**, 60–65 (2006).

123. de Carvalho, R. V. H. *et al.* Leishmania RNA virus exacerbates Leishmaniasis by subverting innate immunity via TLR3-mediated NLRP3 inflammasome inhibition. *Nat. Commun.* **10**, 5273 (2019).

124. Altan-Bonnet, N. Extracellular vesicles are the Trojan horses of viral infection. *Curr. Opin. Microbiol.* **32**, 77–81 (2016).

125. Atayde, V. D. *et al.* Exploitation of the Leishmania exosomal pathway by Leishmania RNA virus 1. *Nat. Microbiol.* **4**, 714–723 (2019).

126. Yoon, Y. J., Kim, O. Y. & Gho, Y. S. Extracellular vesicles as emerging intercellular communicasomes. *BMB Rep.* **47**, 531–539 (2014).

127. Buzás, E. I., Tóth, E. Á., Sódar, B. W. & Szabó-Taylor, K. É. Molecular interactions at the surface of extracellular vesicles. *Semin. Immunopathol.* **40**, 453–464 (2018).

128. Synowsky, S. A. *et al.* The major histocompatibility complex class I immunopeptidome of extracellular vesicles. *J. Biol. Chem.* **292**, 17084–17092 (2017).

129. Théry, C. *et al.* Minimal information for studies of extracellular vesicles 2018 (MISEV2018): a position statement of the International Society for Extracellular Vesicles and update of the MISEV2014 guidelines. *J. Extracell. Vesicles* **7**, 1535750 (2018).

130. Brennan, K. *et al.* A comparison of methods for the isolation and separation of extracellular vesicles from protein and lipid particles in human serum. *Sci. Rep.* **10**, 1039 (2020).

131. Cole, J. L., Lary, J. W., P Moody, T. & Laue, T. M. Analytical ultracentrifugation: sedimentation velocity and sedimentation equilibrium. *Methods Cell Biol.* **84**, 143–179 (2008).

132. Jeppesen, D. K. *et al.* Comparative analysis of discrete exosome fractions obtained by differential centrifugation. *J. Extracell. vesicles* **3**, 25011 (2014).

133. Renner, T. M., Bélanger, K. & Langlois, M.-A. Selective Isolation of Retroviruses from Extracellular Vesicles by Intact Virion Immunoprecipitation. *Bio-protocol* **8**, e3005 (2018).

134. Yu, L.-L. *et al.* A Comparison of Traditional and Novel Methods for the Separation of Exosomes from Human Samples. *Biomed Res. Int.* **2018**, 3634563 (2018).

135. Li, K., Wong, D. K., Hong, K. Y. & Raffai, R. L. Cushioned-Density Gradient Ultracentrifugation (C-DGUC): A Refined and High Performance Method for the Isolation, Characterization, and Use of Exosomes. *Methods Mol. Biol.* **1740**, 69–83 (2018).

136. Onódi, Z. *et al.* Isolation of High-Purity Extracellular Vesicles by the Combination of Iodixanol Density Gradient Ultracentrifugation and Bind-Elute Chromatography From Blood Plasma . *Frontiers in Physiology* vol. 9 1479 (2018).

137. Duong, P., Chung, A., Bouchareychas, L. & Raffai, R. L. Cushioned-Density Gradient Ultracentrifugation (C-DGUC) improves the isolation efficiency of extracellular vesicles. *PLoS One* **14**, e0215324–e0215324 (2019).

138. Mol, E. A., Goumans, M.-J., Doevendans, P. A., Sluijter, J. P. G. & Vader, P. Higher functionality of extracellular vesicles isolated using size-exclusion chromatography compared to ultracentrifugation. *Nanomedicine Nanotechnology, Biol. Med.* **13**, 2061–2065 (2017).

139. Kreimer, S. & Ivanov, A. R. Rapid Isolation of Extracellular Vesicles from Blood Plasma with Size-Exclusion Chromatography Followed by Mass Spectrometry-Based Proteomic Profiling. *Methods Mol. Biol.* **1660**, 295–302 (2017).

140. Sidhom, K., Obi, P. O. & Saleem, A. A Review of Exosomal Isolation Methods: Is Size Exclusion Chromatography the Best Option? *Int. J. Mol. Sci.* **21**, 6466 (2020).

141. Stranska, R. *et al.* Comparison of membrane affinity-based method with size-exclusion chromatography for isolation of exosome-like vesicles from human plasma. *J. Transl. Med.* **16**, 1 (2018).

142. Yang, D. *et al.* Progress, opportunity, and perspective on exosome isolation - efforts for efficient exosome-based theranostics. *Theranostics* **10**, 3684–3707 (2020).

143. Renner, T. M., Tang, V. A., Burger, D. & Langlois, M.-A. Intact Viral Particle Counts Measured by Flow Virometry Provide Insight into the Infectivity and Genome Packaging Efficiency of Moloney Murine Leukemia Virus. *J. Virol.* (2019) doi:10.1128/jvi.01600-19.

144. Busatto, S. *et al.* Tangential Flow Filtration for Highly Efficient Concentration of Extracellular Vesicles from Large Volumes of Fluid. *Cells* **7**, 273 (2018).

145. Carnino, J. M., Lee, H. & Jin, Y. Isolation and characterization of extracellular vesicles from Broncho-alveolar lavage fluid: a review and comparison of different methods. *Respir. Res.* **20**, 240 (2019).

146. Nordin, J. Z. *et al.* Ultrafiltration with size-exclusion liquid chromatography for high yield isolation of extracellular vesicles preserving intact biophysical and functional properties. *Nanomedicine Nanotechnology, Biol. Med.* **11**, 879–883 (2015).

147. Hartjes, T. A., Mytnyk, S., Jenster, G. W., van Steijn, V. & van Royen, M. E. Extracellular Vesicle Quantification and Characterization: Common Methods and Emerging Approaches. *Bioeng. (Basel, Switzerland)* **6**, 7 (2019).

148. Zamora, J. L. R. & Aguilar, H. C. Flow virometry as a tool to study viruses. *Methods* **134**–**135**, 87–97 (2018).

149. McKinnon, K. M. Flow Cytometry: An Overview. *Curr. Protoc. Immunol.* **120**, 5.1.1-5.1.11 (2018).

150. Morales-Kastresana, A. *et al.* Labeling Extracellular Vesicles for Nanoscale Flow Cytometry. *Sci. Rep.* **7**, 1878 (2017).

151. Brittain 4th, G. C. *et al.* A Novel Semiconductor-Based Flow Cytometer with Enhanced Light-Scatter Sensitivity for the Analysis of Biological Nanoparticles. *Sci. Rep.* **9**, 16039 (2019).

152. Headland, S. E., Jones, H. R., D'Sa, A. S. V, Perretti, M. & Norling, L. V. Cutting-edge analysis of extracellular microparticles using ImageStream(X) imaging flow cytometry. *Sci. Rep.* **4**, 5237 (2014).

153. Vogel, R. *et al.* A standardized method to determine the concentration of extracellular vesicles using tunable resistive pulse sensing. *J. Extracell. vesicles* **5**, 31242 (2016).

154. Wright, M. Nanoparticle Tracking Analysis for the Multiparameter Characterization and Counting of Nanoparticle Suspensions BT - Nanoparticles in Biology and Medicine: Methods and Protocols. in (ed. Soloviev, M.) 511–524 (Humana Press, 2012). doi:10.1007/978-1-61779-953-2_41.

155. Bachurski, D. *et al.* Extracellular vesicle measurements with nanoparticle tracking analysis - An accuracy and repeatability comparison between NanoSight NS300 and ZetaView. *J. Extracell. vesicles* **8**, 1596016 (2019).

156. 2020 Particle Metrix GmbH. Introduction to Nanoparticle Tracking Analysis (NTA). 1 https://www.particle-metrix.de/en/technologies/nanoparticle-tracking/articles-nanoparticle-tracking/introduction-to-nanoparticle-tracking-analysis-nta (2020).

157. Helwa, I. *et al.* A Comparative Study of Serum Exosome Isolation Using Differential Ultracentrifugation and Three Commercial Reagents. *PLoS One* **12**, e0170628 (2017).

158. Roingeard, P., Raynal, P.-I., Eymieux, S. & Blanchard, E. Virus detection by transmission electron microscopy: Still useful for diagnosis and a plus for biosafety. *Rev. Med. Virol.* **29**, e2019–e2019 (2019).

159. Winey, M., Meehl, J. B., O'Toole, E. T. & Giddings Jr, T. H. Conventional transmission electron microscopy. *Mol. Biol. Cell* **25**, 319–323 (2014).

160. Ludwig, N. *et al.* Simultaneous Inhibition of Glycolysis and Oxidative Phosphorylation Triggers a Multi-Fold Increase in Secretion of Exosomes: Possible Role of 2′,3′-cAMP. *Sci. Rep.* **10**, 6948 (2020).

161. Zimmermann, J., Radbruch, A. & Chang, H.-D. A Ca(2+) concentration of 1.5 mM, as present in IMDM but not in RPMI, is critical for maximal response of Th cells to PMA/ionomycin. *Eur. J. Immunol.* **45**, 1270–1273 (2015).

162. Savina, A., Furlán, M., Vidal, M. & Colombo, M. I. Exosome release is regulated by a calcium-dependent mechanism in K562 cells. *J. Biol. Chem.* (2003) doi:10.1074/jbc.M301642200.

163. Yi, J. S., Cox, M. A. & Zajac, A. J. T-cell exhaustion: characteristics, causes and conversion. *Immunology* **129**, 474–481 (2010).

164. Kwon, D.-N., Lee, Y.-K., Greenhalgh, D. G. & Cho, K. Lipopolysaccharide stress induces cell-type specific production of murine leukemia virus type-endogenous retroviral virions in primary lymphoid cells. *J. Gen. Virol.* **92**, 292–300 (2011).

165. Flórez-Vargas, O. *et al.* Bias in the reporting of sex and age in biomedical research on mouse models. *Elife* **5**, e13615 (2016).

166. Treger, R. S. *et al.* The Lupus Susceptibility Locus Sgp3 Encodes the Suppressor of Endogenous Retrovirus Expression SNERV. *Immunity* **50**, 334-347.e9 (2019).

Curriculum Vitae

EDUCATION

University of Ottawa, Ottawa, ON
MSc., Biochemistry Microbiology and Immunology **September 2018 - Current**
In progress - Thesis "Characterization of the Immune Stimulated Release of Extracellular Vesicles from Murine Cells "

Bishop's University, Lennoxville, QC
Honours, BSc., Biology **September 2014 – April 2018**
Honors Research project at Université de Sherbrook, in the Raymund Wellinger lab, Sherbrooke, QC.

Town Centre Private High School, Markham, ON September 2013 – June 2014
Bill Crothers Secondary School, Markham, ON September 2010 – June 2013
Ontario Secondary School Diploma **June 2014**

AWARDS

University of Ottawa Graduate Admissions Scholarship September 2018 – August 2020

Honour Roll Scholarships, Bishop's University
- Foundation Scholarship September 2017 – April 2018
- Florence May Foreman Scholarship September 2016 – April 2017

1st place poster presentation in Biochemistry and Cellular Biology, Université de Sherbrooke September 2017

RELATED RESEARCH EXPERIENCE

University of Ottawa, Dr. Marc-Andre Langlois Lab,
Department of Biochemistry, Microbiology and Immunology
MSc Candidate **May 2017 – August 2017**
MSc Project "Characterization of the Immune Stimulated Release of Extracellular Vesicles from Murine Cells"
Conducted research into the distinct immune stimulating conditions where murine naïve CD4+ T-cells would secrete various particles in distinctive egress profiles. The intent of the project was to enable the characterized profiles of particles to be correlated with specific stimulated immune pathways.
- Managed the lab's mouse colony and facilitated spleen extractions in conjunction with the University's ACVS (Animal Care Veterinary Services) guidelines, processes and procedures.
- Proficient in laboratory techniques such as: proper cell culture practices, transfections, infections, stained and labelled cells and supernatants for flow cytometric analyses, cloning by restriction digest, bacterial transformation, plasmid purification, PCR, genomic DNA extractions, RNA extractions, qPCR, prepared supernatants for nanoparticle tracking analysis, Western blotting, ultracentrifugation, and prepared cell samples for fluorescence microscopy.
- Attended presentations, talks, symposia, and student "work in progress" presentations.

- Responsible for maintaining safe laboratory environment. Coordinated collection requests for liquid waste. Collected and ensured solid biohazard waste was disposed of in accordance with departmental guidelines. Maintained inventory on commonly used lab solvents and solutions.
- Utilized laboratory and analytic software such as: Vector NTI, Snap Gene, Quant Studio, GE Image Quant, Viia 7, FlowJo, Graph Pad Prism, ZetaView BASIC NTA, BD FACS Diva, ZEN.

Université de Sherbrooke, Raymund Welllinger Lab
Honours BSc., Research Project **September 2017 – April 2018**

Managed an individual research project in collaboration with Raymund Wellinger's Telomere Biology lab at the Université de Sherbrooke.
Université de Sherbrooke, Raymund Welllinger Lab

Summer Student Internship **May 2017 – August 2017**

- Managed an individual research project, in collaboration with Raymund Wellinger's Telomere Biology Lab at the Université de Sherbrooke, to develop sequences to generate novel telomerase RNA secondary structures.
- Applied common molecular biology techniques such as: cloning techniques (Gibson assembly and Restriction Digest), PCR, Southern Blotting & DNA purification techniques.
- Prepared samples and slides for manipulation with a fluorescence microscope.
- Utilized lab research software: SnapGene, ZEN, NanoDrop, etc. Collaborated with supervisors and colleagues to plan and develop strategies to ensure systematic and organized progression of the project.
- Maintained cleanliness of the lab and availability of lab resources.
- Presented project updates at laboratory meetings to inform associates of new developments and obtain essential critique and feedback for incorporation in the project.

OTHER WORK EXPERIENCE

Town of Richmond Hill, Richmond Hill, ON
Summer Student, Parks Operations **July 2016 – September 2016**

City of Markham, Markham, ON
Swimming Instructor **June 2016 – September 2016**
Lifeguard **April 2016 – September 2016**

PRESENTATIONS

BMI Departmental Poster Day May 2019
Master's Seminar Digital Presentation May 2020

LANGUAGES

English: native language, written and spoken.
French: working knowledge.

SKILLS AND COMPETENCIES

Teamwork

Well-developed teamwork competencies with the ability to work cooperatively and collaboratively with other lab members to achieve team strategies, objectives and successes. Able to work independently and remotely, as needed.

Communication

Well-developed verbal and written abilities.
Advanced presentation skills with the ability to present research material in a clear, concise and easy to understand manner.
Experienced in presenting graduate level courses and research to university researchers and fellow graduate students.
Able to clearly present project updates at laboratory meetings to inform the broader lab team of new developments and obtain essential critique and feedback to incorporate into current research.

Health and Safety

Proficient in Workplace Hazardous Material Information System (WHMIS), as relates to lab safety at the University of Ottawa, and applicability to working in laboratories. Attended and completed required Principles of Biosafety workshops and relevant workplace training.

Computer

Proficient in Windows, Mac OSX, MS Office suite (Word, Powerpoint, Excel), Internet (Edge, Chrome, Explorer, Mozilla, etc.), R-Studio, Graph Pad Prism, FlowJo, BD FACSDiva.

Licensing and Usage

	Basic (Free) Account*	Academic Subscription	Industry Subscription
Educational Uses:			
Academic poster	✓	✓	✓
Thesis/dissertation (unpublished)	✓	✓	✓
Internal meetings (lab or team)	✓	✓	✓
Conference presentation	✓	✓	✓
Assignment/exam	✓	✓	✓
Teaching slides	✓	✓	✓
Personal blog/website posts	✓	✓	✓
Personal social media posts	✓	✓	✓
Publishing Uses:			
Journal publication		✓	✓
Textbook publication (< 5 figures)		✓	✓
Published thesis		✓	✓
Commercial Uses:			
Any uses that generate profit			✓
Textbook publication (5+ figures)			✓
Trade show materials (e.g. brochures)			✓
Information packages/user guides			✓

*Watermark must be included in exported figure
*Free trial on a premium plan recommended for print uses
For use cases not listed here, please go to **biorender.com/contact**

Conditions for Publication rights:

1. The figure was exported under a **paid subscription.**
2. Citation of "**Created with BioRender.com**" appears somewhere in the publication.

$180.00

SUMMARY

To anorr066@uottawa.ca
From Science Suite Inc - o/a BioRender

ITEMS

MARCH 17, 2021 - MARCH 17, 2022

Student Plan Annual (Charged in USD) $180.00
Qty 1

Amount due $180.00

Questions? Contact Science Suite Inc - o/a BioRender

All BioRender-made figures must be cited with

Created with BioRender

Thanks for using BioRender!